Thallium-rich pyrite ores from the Apuan Alps, Tuscany, Italy: constraints for their origin and environmental concerns

Massimo D'Orazio[a], Cristian Biagioni[a*], Andrea Dini[b], Simone Vezzoni[a]

[a]*Dipartimento di Scienze della Terra, Università di Pisa, Via S. Maria 53, 56126 Pisa, Italy*
[b]*Istituto di Geoscienze e Georisorse, CNR, Via Moruzzi 1, 56124 Pisa, Italy*

[*]Corresponding author.
E-mail address: biagioni@dst.unipi.it
Phone: +39 0502215700, *Fax*: +39 0502215800

ABSTRACT

The southern sector of the Apuan Alps (AA) massif, Tuscany, Italy, is characterized by the occurrence of a series of baryte – pyrite – iron oxide orebodies whose Tl-rich nature was recognized only recently. The geochemistry of the pyrite ore was investigated through inductively coupled plasma mass spectrometry. In addition, lead isotope data for selected pyrite ores from AA were collected. Pyrite ores are characterized by a complex geochemistry, with high concentrations of Tl (up to 1100 μg/g) coupled with high As and Sb contents; the Co/Ni ratio is always < 1. Geochemical data of pyrite and marcasite ore samples from other mining districts of Tuscany have been collected in order to compare them with those from the AA. These samples usually have very low Tl content (less than 2 μg/g) and high to very high Co/Ni and As/Sb ratios. Only some samples from the Sb-Hg ore deposits showed very high Tl concentrations (up to ~ 3900 μg/g). Another difference is related to the lead isotope composition, with pyrite ores from AA markedly less radiogenic than those from the other deposits from Tuscany. Geochemical data of pyrite ores from AA give new insights on the genesis of the baryte – pyrite – iron oxide orebodies, relating their formation to low temperature hydrothermal systems active during early Paleozoic; in addition, these data play a fundamental role in assessing the environmental impact of these deposits.

Keywords: thallium, pyrite, geochemistry, environmental impact, Apuan Alps, Tuscany.

Introduction

Thallium (Tl) is a relatively rare heavy element occurring in the upper continental crust at an average concentration of 0.75 µg/g (Wedepohl 1995), and at even lower concentrations in the other major solid Earth reservoirs. Thallium does not commonly form concentrations at geological scale, but occurs dispersed mainly within feldspars and feldspathoids, micas, clay minerals, and within sulfides. Indeed, Tl has both a lithophile and chalcophile geochemical behavior. Thallium may also occur at high concentrations in Fe-Mn nodules (Iskowitz et al. 1982; Hein et al. 2000; Rehkämper et al. 2004) and hot spring deposits from epithermal settings (e.g., Krupp and Seward 1990). This element is mainly extracted as a by-product of the smelting or refinement of Zn, Pb, Cu, Hg, As, and Fe sulfides. Ores mined specifically for Tl currently occur only in some Chinese localities (Zhou et al. 2005).

Over the last two decades, the scientific interest for Tl has greatly increased because it was more and more recognized as a very toxic substance for humans and many other living organisms (e.g., Peter and Viraraghavan 2005, and reference therein), and because it found use in many high-tech scientific and industrial applications (Nriagu 1998). Thallium exists in two naturally occurring oxidation states, monovalent Tl(I) and trivalent Tl(III). According to the thermochemical data (e.g., Xiong 2007), Tl(I) should be the dominant oxidation state for this element in the majority of natural environments. However several studies demonstrated that Tl(III) species could be stabilized as anionic complexes with Cl^- or OH^- anions (Batley and Florence 1975). Thallium(I) can be also oxidized to Tl(III) by the action of Tl-oxidizing bacteria or by UV or sunlight irradiation (Karlsson et al. 2006). The knowledge of Tl speciation is important because Tl(III) compounds should have toxicological effects different from those of Tl(I) compounds (Ralph and Twiss 2002), and because the mobility of this element in the environment varies as a function of its oxidation state (e.g., Xiong 2007).

Following the first identification of Tl sulfosalts in the baryte – pyrite – iron oxide deposits from the southern Apuan Alps (hereafter AA; Orlandi et al. 2012, 2013), and the discovery of the exceptional Tl mineralization associated with these orebodies (Biagioni et al. 2013), a geochemical investigation of the pyrite ores was mandatory, owing to the Tl-rich nature of several pyrite occurrences world-wide, e.g., the Xiangquan thallium deposit, eastern China (Zhou et al. 2005), and to the common association of Tl with other potentially toxic heavy metals and metalloids (e.g., As, Cd, Hg) within pyrite (Deditius and Reich 2016). Accordingly, we performed a more detailed geochemical survey of the pyrite ores from southern AA, and a comparison with new data collected on pyrite/marcasite ores from other mining districts of Tuscany (Fig. 1). Tuscany was indeed one

of the few Italian regions that experienced a significant mining activity. Even though this activity definitively ceased at the end of the '80s of the XX century, it left a legacy of environmental problems, mostly related to acid mine drainage (AMD). In fact, a significant fraction of mining activity in Tuscany was concentrated on the extraction of pyrite, exploited for the production of sulphuric acid, or other minerals (hematite, magnetite, iron hydroxides, sphalerite, galena, chalcopyrite, cinnabar, stibnite, baryte, etc.) associated to large masses of unwanted pyrite and/or marcasite.

The aims of this study are (i) to document the abundance of Tl and associated elements in the pyrite ores from the southern AA, (ii) to determine their Pb-isotope signature, (iii) to give constraints to the origin of this Tl mineralization, and (iv) to evaluate which of the abandoned mines from the whole Tuscany could represent a potential source of Tl contamination *via* the release of AMD following pyrite/marcasite oxidation.

The baryte – pyrite – iron oxide ore deposits from southern Apuan Alps

General features

The AA represent the largest tectonic window of the Northern Apennines and are composed by the stacking of different tectonic units (e.g., Fellin et al. 2007 and reference therein). The lowermost ones, i.e. the Apuane and Massa units, were affected by regional metamorphism under moderate-pressure greenschist facies conditions during late Oligocene – early Miocene. Several kinds of ore deposits are hosted within these metamorphic units. Based on their mineralogy and elemental associations, Lattanzi et al. (1994) distinguished at least eight different types. One of the most important is represented by a series of baryte – pyrite – iron oxide orebodies aligned along a ~ 10 km SW-NE discontinuous mineralized belt located in the southern portion of the AA massif (Fig. 2). The geological setting, mineralogy, and geochemistry of these deposits have been described in several papers (e.g., Carmignani et al. 1975, 1976; Cortecci et al. 1985; Orberger et al. 1986; Costagliola et al. 1990; Benvenuti et al. 1990; Cortecci et al. 1992; Lattanzi et al. 1994; Costagliola et al. 1998) and only some general outlines will be given here.

The main orebodies were exploited in the Pollone, Monte Arsiccio, Canale della Radice, Buca della Vena, and Fornovolasco mines (Fig. 2). All these orebodies share several features:

1) they present stratiform, near-conformable, lens-shaped morphologies (Fig. 3a) and are hosted within or close to a Paleozoic phyllitic complex containing lenses or beds of quartzites and carbonates (Fig. 3b), especially in its upper portion near the contact with the Triassic metadolostone of the *Grezzoni* Formation;

2) they are characterized by a simple primary mineralogy (baryte, pyrite, hematite, magnetite);

3) they generally show a distinct mineral zoning reflecting changes in the host rock lithology, with pyrite ± baryte mainly located within the phyllitic rocks at the footwall of the orebodies, and iron oxide ± baryte mainly occurring near the contact with the metadolostones at the hanging wall of the ores;

4) the Paleozoic phyllitic complex hosting the orebodies is characterized by the widespread occurrence of tourmalinite rocks (Fig. 3c). Tourmalinite is also common in the Pb-Ag-Zn ore deposits from the Bottino–Gallena area, where they have been known since early mining reports and were used by the miners as a prospective tool. Benvenuti et al. (1989) hypothesized a pre-metamorphic, probably sedimentary-exhalative, nature of the tourmalinite bodies from the Bottino deposit;

5) they are spatially associated to Lower Paleozoic meta-rhyolite rocks. These rocks also occur in other ore deposits from the southern AA (e.g., Bottino and Argentiera di Sant'Anna mines);

6) the orebodies show evidence of metamorphic deformation and/or recrystallization, from micro- to macroscale. These deformative features are enhanced by the banded textures displayed by several orebodies (Pollone, Monte Arsiccio, Buca della Vena), showing the alternation of baryte + pyrite and baryte + iron oxides (Fig. 3d). On the contrary, at the Canale della Radice and Fornovolasco mines the lens-shaped bodies are usually mono-mineralic, being predominantly composed of pyrite or magnetite, with baryte occurring just as an accessory mineral. Discordant bodies are typically subordinate and have been interpreted as the products of metamorphic remobilization from the stratiform ores (e.g., Cortecci et al. 1992) or as the result of the circulation of hydrothermal fluids deriving from deeper structural levels (e.g., Costagliola et al. 1998).

The genesis of these ore deposits is controversial and two main genetic models have been so far proposed. According to Carmignani et al. (1972, 1976), the deposits are the result of the replacement of carbonate rocks by fluids related to a hypothetical synkinematic granitic intrusion of Tertiary age, with mineralizing fluids able to rise just along the most important shear zones occurring in the southern sector of the AA. As a matter of fact, up to date no evidence of Tertiary magmatism has been found in the AA.

Since Bergmann (1969), who hypothesized a Permo-Triassic exhalative origin for these deposits, several authors (e.g., Ciarapica et al. 1985; Cortecci et al. 1985; Benvenuti et al. 1986; Costagliola et al. 1990) proposed that the orebodies formed during middle-late Triassic as sedimentary-diagenetic proto-ores in a near-shore

environment, subsequently metamorphosed and partly remobilized during the Apennine orogeny. A synsedimentary origin was proposed also by Orberger et al. (1986) but these authors suggested a Silurian-Devonian age for the mineralization.

In order to constrain the possible source of metals of the ore deposits from southern AA, Lattanzi et al. (1992) determined the Pb-isotope compositions of pyrite, galena, meneghinite, baryte, and country rocks from several orebodies, including the Monte Arsiccio and Pollone ones. They concluded that a major episode of Pb concentration, possibly related to the formation of exhalative tourmalinites, may have occurred at 350-400 Ma. The Paleozoic Pb was later reworked during the late Tertiary Apennine orogeny.

Indeed, the main orebodies show evidences of a pre-Apennine origin. They suffered a mineralogical and textural reorganization during the Tertiary tectono-metamorphic events, when hydrothermal fluids, as well as minor sulfide melts, favoured the *in situ* remobilization of these orebodies, forming localized concentrations of sulfides and sulfosalts in late-stage extension veins and along grain boundaries of the baryte + pyrite orebodies (Biagioni et al. 2013, 2016).

The thallium-rich pyrite ores

The mineralized bodies were exploited up to the end of 1980s; they were formerly mined for iron oxides for iron production, and subsequently for baryte and mixed baryte-magnetite-hematite used as weighting agents in petroleum well drilling mud. Pyrite was discontinuously exploited for the production of sulphuric acid. The volume and geometry of the mineralized masses, as well as the relative proportion of pyrite, baryte, and iron oxides vary greatly in the different mining sites. On the contrary, the nature of the pyrite ore is poorly variable (Carmignani et al. 1976): pyrite ore occurs both as nearly monomineralic granular masses forming lens-shaped bodies (Fig. 3a), and as deformed centimetric bands alternating with baryte (Fig. 3d) and locally with tourmalinite. The occurrence of idiomorphic crystals of pyrite in late-stage Alpine veins can be considered negligible.

As stated above, the baryte – pyrite – iron oxide orebodies are mineralogically zoned. Typically, pyrite occurs in the lowermost portion of the orebodies, near the contact or within the phyllitic complex. Upwards, the content of baryte may increase and the orebodies assume a banded texture, largely parallel to the main field schistosity and affected by folding. There is a continuous transition between the orebodies and the sub-economic baryte – pyrite layers within the country rocks. Recent field study of the Pollone deposit indicates that the baryte-

pyrite lenses/layers hosted by the Paleozoic metamorphic formations suffered intense deformation and folding during the Apennine deformation event (Biagioni et al. 2016).

Under the microscope, pyrite ores are mainly formed by pyrite, usually associated with low amounts of other sulfides and gangue minerals. Two generations of pyrite have been recognized by former authors (e.g., Natale 1974): the first one is constituted by very small (1-5 μm) equant and anhedral crystals, whereas the second generation is represented by larger (10-500 μm) idiomorphic cubic or pyritohedral crystals. The transition between the two generations is gradual and it is very well emphasized by etching polished pyrite surfaces with a weak acid solution as done by Natale (1974). Etched idiomorphic pyrite crystals show strongly zoned and anhedral cores characterized by low crystallinity, surrounded by thick homogeneous and highly crystalline rims. The same author reported the occurrence of framboidal pyrite aggregates 20-30 μm in size.

The present textures are the result of the metamorphic recrystallization of the orebodies. In fact, despite its hardness and its generally refractory nature, pyrite tends to recrystallize starting from greenschist facies conditions (e.g., Craig and Vokes 1993). Several authors estimated *P-T* conditions suffered by the AA metamorphic complex during the Apennine orogeny. For example, Costagliola et al. (1998) reported *P-T* conditions of 350 °C and 0.35 GPa on the basis of chlorite and arsenopyrite geothermometers and phengite geobarometer, respectively, for the host rocks of the Pollone ore deposit, whereas appreciably higher temperatures (around 450 °C) were found for the mineralizing fluids at the same locality.

The thallium-rich nature of the pyrite ores from southern AA was recognized only recently (Biagioni et al. 2013) and it was completely unnoticed during mining works and the subsequent geological studies. In particular, the Tl mineralization of the Monte Arsiccio mine consists of up to ≈ 390 μg/g Tl in microgranular pyrite coupled with the occurrence of macroscopic thallium sulfosalts within different host rocks (i.e., baryte + pyrite orebodies, pyrite-rich metadolostones, and quartz + baryte + carbonate veins; Fig. 4), and the occurrence of Tl-rich varieties of Pb-Sb-As sulfosalts (e.g., Biagioni et al. 2014c). As evidenced by Biagioni et al. (2013), the Tl sulfosalts assemblages from the Monte Arsiccio mine show textural evidence (e.g., migration along matrix grain boundaries, drop-like internal textures, low interfacial angles between sulfosalts and matrix minerals) for their mobilization as low-temperature (300-450 °C) melts.

Samples and analytical methods

A total of sixty-three representative pyrite/marcasite ore samples from Tuscany (Table 1) was analyzed. Each sample from AA consists of at least 1 kg of bulk pyrite ore and represents the most common sulfide-ore of each mineralization. Twenty-seven samples were collected in the following baryte – pyrite – iron oxide abandoned mines of the southern AA (Lucca province): Pollone (Valdicastello Carducci, Pietrasanta), Monte Arsiccio (Sant'Anna di Stazzema, Stazzema), Canale della Radice (Mulina di Stazzema, Stazzema), Buca della Vena (Pontestazzemese, Stazzema), and Fornovolasco (Fabbriche di Vergemoli). The series of samples from the AA orebodies is completed by three samples of microgranular pyrite ore from the Ribasso Santa Barbara and Fontana tunnels, Argentiera di Sant'Anna mine (Sant'Anna di Stazzema, Stazzema), by a sample of microgranular pyrite ore from the galena prospect of La Tana (Cardoso, Stazzema), and one sample of microcrystalline pyrite + baryte from an ore-rock outcrop located along the road from Sant'Anna di Stazzema to Case Sennari. The mineralogy of these samples was investigated through X-ray powder diffraction (XRD), reflected-light microscopy, micro-Raman spectrometry, and scanning electron microscopy (SEM). The pyrite ores often contain a significant fraction of gangue minerals, represented by baryte and, subordinately, by quartz ± carbonates ± phyllosilicates. Some samples from the Fornovolasco, Canale della Radice and Argentiera di Sant'Anna mines contain a small fraction (< 5 wt%) of mackinawite/pyrrhotite ± arsenopyrite.

Twenty-four samples were collected from several Fe and base metal deposits from southern Tuscany and Elba Island, whereas seven are from the Hg-Sb ores of Monte Amiata and Manciano areas (Table 1). These samples are constituted almost exclusively by pyrite (plus marcasite for the Hg-Sb deposits) with only minor amounts of gangue minerals, represented by quartz ± carbonates ± adularia ± chlorite. Reviews on the ore deposits from these mining districts have been given by several authors, e.g., Tanelli et al. (2001), Dini (2003), Rimondi et al. (2015).

About 50 mg of freshly-grinded pyrite/marcasite bulk ore powders were dissolved with 4 ml concentrated HNO_3 (Romil SuperPure) in perfluoralkoxy (PFA) vials. After appropriate dilution with ultrapure water (Millipore Milli-Q, > 18.2 MOhm cm), the sample solutions were analyzed for V, As (kinetic energy discrimination mode; cell gas = 3.7 ml/min He) and Mn, Co, Ni, Cu, Zn, Mo, Ag, Cd, Sb, Tl, Pb (standard mode), with a Perkin Elmer NexION 300X inductively coupled plasma mass spectrometer (ICP-MS) at the Pisa University's Dipartimento di Scienze della Terra. A solution containing 20 ng/ml of Rh and Re (internal standards) was mixed on-line with the sample solution just before reaching the nebulizer. The instrument was calibrated with synthetic solutions made by diluting and mixing 10 µg/ml single element stock solutions (Inorganic Ventures). Analyte masses and detection limits are reported in Table 2. The approximate amount of

gangue minerals in each sample was estimated by determining the concentrations of Fe, Ba, Ca, Si, Al, and Sr using a NITON XL3t GOLDD+ energy-dispersive X-ray fluorescence (ED-XRF) hand-held spectrometer. In particular, the amount of baryte in the pyrite ore samples from the AA was obtained calibrating the ED-XRF spectrometer with mixtures of variable proportions of pure baryte + pyrite.

The Pb-isotope compositions of selected samples of pyrite ores, galena, and sulfosalts from the southern AA were determined at Istituto di Geoscienze e Georisorse-CNR, Pisa, using a Finnigan MAT 262 multicollector mass-spectrometer operating in static mode, with conventional extraction by chromatographic ion exchange in Dowex 1 anion resin, using standard HBr and HCl elution procedures. Replicate analyses of Pb isotope ratios are accurate to within 0.025% (2SD) per mass unit, after applying mass discrimination corrections of 0.15 ± 0.01% per mass unit relative to the NIST SRM 981 reference composition of Todt et al. (1993). Lead blanks were on the order of 0.2-0.4 ng during the period of chemistry processing, and no blank correction was made.

The identification of some uncertain minerals was performed through X-ray powder diffraction using a Bruker D2 Phaser diffractometer (30 kV, 10 mA) operating in Bragg-Brentano geometry (θ-θ scan mode) and equipped with a 1-dimensional Lynxeye detector. Ni-filtered Cu *K*α radiation was used. Data were collected in the scan range 4-65° in 2θ, with scan step of 0.02° and counting times of 0.1 s/step. Data were processed through the software Diffrac.Eva (Bruker AXS).

In order to identify accessory phases, the pyrite ores from Apuan Alps were further characterized using a Philips XL30 scanning electron microscope equipped with an EDAX DX4 detector and through micro-Raman spectrometry, collecting unpolarized micro-Raman spectra in nearly back-scattered geometry with a Jobin-Yvon Horiba XploRA Plus apparatus, equipped with a motorized x-y stage and an Olympus BX41 microscope with a 100 × objective. The Raman spectra were excited by a 532 nm light of a solid state laser attenuated to 10%.

Results

Apuan Alps

Pyrite ores from the baryte – pyrite – iron oxide orebodies of the southern AA examined in this study (Fig. 5) show different mineralogy from one deposit to the other, even if pyrite is always the most abundant mineral. In agreement with previous authors (e.g., Natale 1974), pyrite forms either xenoblastic or idioblastic (cubic or

pyritohedral) individuals, with size ranging from few μm to ~500 μm (Fig. 5a). In some samples, growth zoning has been observed.

Associated minerals represent only a minor fraction of the pyrite ores and they usually occur as interstitial grains in the pyrite ore; only rarely some μm-sized grains have been observed as inclusion in pyrite crystals. These minerals can be divided in accessory ore minerals and gangue minerals.

Accessory ore minerals do not occur in all the samples studied. Indeed, the sample from Sennari and some samples from Argentiera di Sant'Anna do not show any evidence of the occurrence of other sulfides than pyrite (Fig. 5b). The ore minerals are represented mainly by sulfides, i.e. arsenopyrite, chalcopyrite, galena, mackinawite, pyrrhotite, sphalerite, stibnite, ullmannite, tetrahedrite, and some rare sulfosalts. Arsenopyrite was observed in samples from Fornovolasco and Canale della Radice. Whereas in the latter samples this sulfide is very rare, being observed only once, in those from Fornovolasco arsenopyrite frequently occurs as idioblastic to subidioblastic crystals, up to 50 μm (Fig. 5c), associated with xenoblastic mackinawite. In the same samples, minor amounts of Fe-rich sphalerite, sometimes forming symplectitic intergrowths with stibnite, have been observed. Sphalerite is the most common accessory sulfide in pyrite ores. In addition to the Fe-rich variety from Fornovolasco, sphalerite has been observed in samples from Canale della Radice (Fe-rich), Pollone, and Monte Arsiccio. Chalcopyrite and ullmannite have been identified in pyrite ore samples from Canale della Radice, whereas galena occurs as interstitial grains or as inclusions in pyrite crystals in ore samples from the Pollone mine (Fig. 5d), associated with the Pb-(Sb/As) sulfosalts (jordanite-geocronite) and Ag-Sb sulfosalts. Other Pb-Sb sulfosalts, in grain less than 5 μm in size, have been observed as inclusions in pyrite crystals from the Fornovolasco pyrite ores, whereas Tl-Pb-(Sb/As) and Tl-Hg-(Ag/Cu)-(As/Sb) sulfosalts occur in veins cross-cutting the pyrite ores or as interstitial grains in the samples from the Monte Arsiccio mine (Fig. 5e). Tetrahedrite has been identified in only some samples from this latter locality.

Locally, ore minerals are represented by oxides too, i.e. V-bearing magnetite identified in pyrite ore samples from the Buca della Vena mine.

Gangue minerals are quartz, fluorite, carbonates, baryte, and phyllosilicates. Quartz is widespread in all the studied samples, whereas fluorite occurs only in pyrite ore samples from the Pollone mine. Carbonates can be represented by siderite (Fornovolasco and Argentiera di Sant'Anna mines), calcite, dolomite (Pollone and Monte Arsiccio mines), and some barium carbonates (Monte Arsiccio mine, Sennari; Fig. 5e,f). Baryte is a widespread accessory mineral in pyrite ore samples from the Pollone, Monte Arsiccio, and Buca della Vena mines, whereas it occurs as rare scattered μm-sized grains in pyrite ores from Fornovolasco, Canale della Radice, Argentiera di

Sant'Anna, and Sennari. Phyllosilicates are particularly abundant in pyrite ores from Canale della Radice, where a V-bearing muscovite has been observed; this variety of muscovite occurs also in the samples from Buca della Vena. Muscovite is also frequent in pyrite ores from the Pollone mine, where it is Ba-enriched. Another phyllosilicate observed in the samples studied is stilpnomelane, identified in pyrite ores from Fornovolasco. Other gangue minerals occasionally observed are scheelite (Fornovolasco), LREE phosphates (Canale della Radice), V-bearing derbylite (Buca della Vena), and a member of the apatite supergroup (Monte Arsiccio, Sennari).

The most important geochemical feature of the microgranular pyrite ore samples from the baryte – pyrite – iron oxide orebodies of the southern AA is represented by their high to very high concentrations of Tl (mostly > 100 µg/g and up to 1110 µg/g; Table 3, Fig. 6), confirming the preliminary data reported in Biagioni et al. (2013). The highest levels of thallium have been found in the magnetite – pyrite mine of Fornovolasco, where the microcrystalline pyrite contains on average ~ 850 µg/g of Tl (from 680 to 1110 µg/g). In the samples from Fornovolasco, high thallium concentrations are accompanied by high contents of As (1240 – 2120 µg/g) and Sb (1260 – 1970 µg/g; Fig. 6a, b), and by high contents of Pb (110 – 300 µg/g). Samples with high Tl contents (440 – 1030 µg/g) also occur in the Canale della Radice mines. Again these samples are characterized by high levels of As and Sb but, in this case, also a remarkably high amount of V (147 – 779 µg/g; Fig. 6c). The other abandoned mines sampled during this study (Pollone, Monte Arsiccio, Argentiera di Sant'Anna, Buca della Vena, and La Tana) show more variable, but still high (> 10 µg/g), contents of Tl. For these samples the bulk concentration of Tl varies as a function of the proportion of baryte, quartz, and carbonates (all containing negligible Tl) associated to pyrite (Table 1).

Taken as a group, the pyrite ores from the southern AA are also characterized by very low to low Co concentrations (from 0.4 to 62 µg/g; average = 12.9 µg/g) coupled with low to moderately high Ni contents (from 9.4 to 458 µg/g; average = 120 µg/g). Their Co/Ni ratios are always < 1. The Sb (from 67 to 2430 µg/g; average = 788 µg/g) and As (from 105 to 2120 µg/g; average = 694 µg/g) contents are high but the As/Sb ratio is mostly < 3.

The Pb-isotope compositions of five pyrite ores, ten galena, and five sulfosalt samples from the southern AA are reported in Table 4. These materials are representative of both the baryte – pyrite – iron oxide orebodies and the galena – sphalerite – chalcopyrite – tetrahedrite – lead sulfosalt mineralizations of the Bottino and Argentiera di Sant'Anna mines. In $^{208}Pb/^{204}Pb$ vs $^{206}Pb/^{204}Pb$ and $^{207}Pb/^{204}Pb$ vs $^{206}Pb/^{204}Pb$ space (Fig. 7a, b), these samples plot in a very limited area between the fields enclosing the base-metal ores from southern Tuscany

(excluding the Jurassic, ophiolite-hosted, Cu deposits; Stos-Gale et al. 1995, Lattanzi et al. 1997), and from Sardinia (Boni and Koeppel 1985; Ludwig et al. 1989; Boni et al. 1992; Dini et al. 2005). Indeed, the Pb-isotope compositions for the ores from southern AA ($^{208}Pb/^{204}Pb$ = 38.48-38.61, $^{207}Pb/^{204}Pb$ = 15.66-15.68, $^{206}Pb/^{204}Pb$ = 18.31-18.43) are markedly less radiogenic than those from southern Tuscany ($^{208}Pb/^{204}Pb$ = 38.84-39.25, $^{207}Pb/^{204}Pb$ = 15.66-15.75, $^{206}Pb/^{204}Pb$ = 18.69-19.21) and slightly more radiogenic than those from Sardinia ($^{208}Pb/^{204}Pb$ = 37.92-38.47, $^{207}Pb/^{204}Pb$ = 15.62-15.68, $^{206}Pb/^{204}Pb$ = 17.86-18.30). More in detail, it can be observed that the sulfosalts and the pyrite ores, particularly those from Monte Arsiccio, have a very slight tendency towards higher $^{208}Pb/^{204}Pb$ and $^{206}Pb/^{204}Pb$ ratios with respect to the galena samples from the other nearby localities (Table 4).

Iron and base metal deposits from southern Tuscany

Notwithstanding the highly variable mode of occurrence (idiomorphic macroscopic crystals, blocky and microcrystalline masses) and the highly variable nature of the associated ore and gangue minerals (e.g., base metal sulfides, hematite, magnetite, carbonates, quartz, adularia, etc.), all the analyzed pyrite ores from southern Tuscany contain very low amounts of Tl (mostly < 0.5 µg/g and up to 2 µg/g; Table 5). The minor- and trace-element signature of these samples is extremely variable. However, with respect to pyrite ores from AA, some significant differences can be stressed. In the three diagrams Co/Ni, As/Sb, and V vs Tl (Fig. 8a, b, c), the pyrite ores from southern AA and southern Tuscany are very clearly separated: samples from southern Tuscany have high to very high Co/Ni (Fig. 8a) and As/Sb (Fig. 8b) ratios coupled with much lower Tl and V contents (Fig. 8c). In addition, pyrite ores from southern Tuscany have extremely low contents of Mo (often below the detection limit of about 0.7 µg/g of the used method).

Mercury-antimony deposits of southern Tuscany

The Hg mineralizations of the Monte Amiata and the Sb mineralizations of the Manciano area (southernmost Tuscany) are frequently associated to masses of pyrite and/or marcasite. Seven samples from six different abandoned mines were analyzed. The results indicate a widely varying geochemistry (Fig. 8a, b, c). A fibrous-radiate pyrite nodule from the Tafone Sb mine is characterized by the highest Tl concentration (3880 µg/g) measured in this work. This sample is also extremely rich in As (6.8 wt%) and Sb (4540 µg/g). Pyrite and

marcasite samples from the Hg mines of Monte Amiata have a very variable Tl content: marcasite from Abbadia San Salvatore, Pietrineri, and Siele mines is rich in Tl (from 80 to 250 µg/g), whereas the mixed pyrite-marcasite sample from the Bagnore mine and the pyrite sample from the Siele mine have both less than 1 µg/g of Tl (0.11 and 0.70 µg/g, respectively). Finally, a sample of mixed pyrite-marcasite crystals from the Monte Labro mine has an intermediate Tl content of 24 µg/g. In terms of Co/Ni and As/Sb ratios, the pyrite/marcasite ores from Monte Amiata and Manciano area do not form a coherent group. Indeed their As/Sb ratios are highly variable but generally above those characterizing the pyrite ores from the AA. The Co/Ni ratios are even more variable: the Tl-rich marcasite from Abbadia San Salvatore, Pietrineri, Siele, and Monte Labro mines have very low Co/Ni ratios (0.01-0.02), comparable to the samples from the AA, while the Tl-poor mixed pyrite-marcasite sample from Bagnore and the pyrite sample from the Siele mine display high Co/Ni ratios.

Discussion

Relationships between geochemistry and mineralogy of pyrite ore from the southern Apuan Alps

The studies on the trace element content of pyrite from several localities world-wide have shown that this common iron disulfide is able to host from µg/g to wt% of heavy metals and metalloids, thus representing both a potential metal resource and an environmental hazard. Unfortunately, only few studies are devoted to the knowledge of metal speciations in pyrite (e.g., Deditius et al. 2008, 2011, 2016). The geochemistry of the pyrite ores from southern AA can be interpreted as due both to elements hosted within the crystal structure of pyrite and to the contribution of accessory minerals occurring in the ore samples.

Thallium, Sb, and As are the elements characterizing the geochemistry of the samples studied. Whereas Tl content in pyrite ores from the Monte Arsiccio mine, ranging from 77 to 393 µg/g, could be at least partially related to the occurrence of thallium sulfosalts (Fig. 5e), samples showing high Tl contents (Fornovolasco, Canale della Radice, and Sennari, with Tl contents up to 1110, 1030, and 624 µg/g) do not show any other sulfide than pyrite. Even if some Tl could replace K in muscovite and stilpnomelane occurring in some of these pyrite ores, it is likely that a significant fraction of this element is associated with pyrite. SEM-BSE observations do not show any evidence of Tl-bearing inclusions down to a sub-micrometer scale. Even if some authors proposed the occurrence of Tl^0 (e.g., Zhou et al. 2005) and Tl^{3+} (e.g., Huston et al. 1995) in pyrite, Tl generally occurs as Tl^+ in sulfides. Consequently thallium could be hosted in pyrite through a coupled substitution Tl^+ +

$(As,Sb)^{3+} = 2Fe^{2+}$. A similar mechanism could be hypothesized to explain the occurrence of other monovalent metals, such as Cu^{+} and Ag^{+}. However, it should be noted that the highest Cu contents in pyrite ores from AA are related to the occurrence, as accessory minerals, of chalcopyrite and tetrahedrite (e.g., in samples from Monte Arsiccio and Canale della Radice). Similarly, the highest Ag contents (e.g., those shown by pyrite ores from the Pollone mine) are due to the presence of Ag-Sb sulfosalts, in some cases included in galena, both as interstitial grains in the pyrite ore or, sometimes, as inclusions in pyrite crystals. In all cases, the analyses plot homogenously above the line representing the atomic ratio (Tl+Cu+Ag)/(As+Sb) = 1 (Fig. 9), in agreement with the results of Deditius et al. (2016).

Arsenic and Sb contents are related not only the above mentioned substitutions, but they could also be hosted in accessory sulfides or they could substitute S in the disulfide anion, forming $(AsS)^{2-}$ or $(SbS)^{2-}$ groups (e.g., Simon et al. 1999). As concern accessory sulfides, the main As and Sb carriers are represented by arsenopyrite and stibnite; minor amounts of Pb-Sb-As sulfosalts have been observed. Arsenopyrite is relatively frequent in samples from Fornovolasco and it was observed also in some samples from Canale della Radice. The corresponding geochemical data collected on the pyrite ores show the highest As contents, i.e. up to 2120 μg/g. Stibnite was observed in samples from Fornovolasco and Monte Arsiccio; indeed, these samples reach the maximum Sb content detected in pyrite ores from southern AA, i.e. up to 2430 μg/g. In addition to the contribution of accessory sulfides, the occurrence of As and Sb in the crystal structure of pyrite cannot be excluded. At the present stage of study, it is not clear which is the oxidation state of As and Sb occurring in pyrite from AA, but the contribution of both pyrite and accessory sulfides to the As and Sb content in pyrite ores can be reasonably assumed.

Manganese, Co, Ni, and possibly Cu^{2+} can show isovalent substitutions for Fe^{2+} in the crystal structure of pyrite, in agreement with the existence of the members of the pyrite group hauerite (MnS_2), cattierite (CoS_2), vaesite (NiS_2), and villamaninite (CuS_2). However, high contents of these elements are related to the presence of accessory sulfides and/or gangue minerals. The very high Mn content measured in a ore sample from Argentiera di Sant'Anna mine (2270 μg/g) is related to the occurrence of Mn-bearing siderite, whereas the high Ni contents shown by samples from Canale della Radice and Fornovolasco could be related to the presence of ullmannite in the former locality and mackinawite (sometimes containing detectable amounts of Ni) in the latter site.

The content of zinc and cadmium seems to be related to the widespread occurrence of sphalerite as accessory sulfide in the pyrite ore. Accurate crystal-chemical data on sphalerite from AA are still lacking and its

Cd contents are not known; however the finding of yellow coatings of greenockite/hawleyite from the Pb-Zn-Ag Bottino ore deposit (authors' unpublished data) agrees with detectable Cd contents in sphalerite (at least locally).

Lead is another divalent metal occurring in pyrite ores from AA. Whereas Deditius et al. (2008) suggested the possible isovalent substitution of Fe^{2+} with Pb^{2+}, the different ionic radius (0.61 Å and 1.19 Å in six-fold coordination for Fe^{2+} and Pb^{2+}, respectively – Shannon 1976) do not support such a hypothesis that deserves further studies. In pyrite ores from AA, the highest contents (10320 μg/g) are related to the occurrence of admixed galena (sample from the Fontana tunnel, Argentiera di Sant'Anna mine) or to the presence of lead-antimony-arsenic sulfosalts (e.g., jordanite-geocronite at the Pollone mine).

Finally, V and Mo are two elements characterizing the pyrite ores from AA with respect to the other Tuscan occurrences. Vanadium sulfides are very rare (only seven mineral species known up to date) and they have been found in only found in few localities. Probably its occurrence in the pyrite ores have to be ascribed to the presence of accessory oxides (magnetite, derbylite), as observed in samples from Buca della Vena, showing up to 252 μg/g, or V-bearing muscovite in V-rich pyrite ores from Canale della Radice (up to 779 μg/g). The high amounts of Mo (up to 59 μg/g in a sample from Fornovolasco; Fig. 6d) are another intriguing geochemical feature of pyrite ores from AA. Usually, pyrite is considered an important sink for marine Mo in anoxic sediments and black shales (e.g., Vorlicek et al. 2004); however recently Chappaz et al. (2014) raised some doubts about this assumption, showing that the role of pyrite as Mo host is subordinate to that played by non-pyritic components within the matrix. Mineralogical data collected on pyrite ore samples only show the occurrence of minor scheelite; this calcium tungstate could indeed host Mo (Hsu and Galli 1973).

In conclusion, the geochemistry of pyrite ores from AA is probably related to the interplay between a complex crystal-chemistry of pyrite (representing the most abundant mineral in the samples studied) and the variable amount and nature of accessory phases. It is worth noting that the present mineralogy and texture of the pyrite ores are the results of a long geological history, even if the observed features are probably related to the recrystallization of the orebodies during the Apennine orogeny and their interactions with hydrothermal fluids, as well as sulfide melts, favouring the *in situ* remobilization of elements and the crystallization of new mineral assemblages in late-stage extension veins/cracks/intergranular voids.

Pyrite ore geochemistry and late-stage extension vein mineralogy: an evidence of *in situ* remobilization

The geochemical data on pyrite ores presented in this paper can be compared with the mineralogy of late-stage Alpine extension veins hosted within these ore deposits. Indeed, these veins, being very small in size and usually being not interconnected, acted as local drainage systems only. Consequently, their infill mirrors the composition of the local host and the physical-chemical features of local fluids, thus representing indicators of late-stage *in situ* remobilization processes (e.g., Biagioni et al. 2016). Consequently, the elemental association characterizing these mineralizations can be defined by coupling geochemical as well as mineralogical data. Besides Fe and Ba, the elements forming the main and largely prevailing ore minerals, other metals/metalloids characterizing these mineralizations are Sb, As, Tl, Hg, the ubiquitous Pb-Ag-Zn triplet, and, very subordinately, V, Ni and Mo.

The most important geochemical fingerprint of the pyrite ores from southern AA is certainly represented by their high Tl contents. Mineralogical studies revealed that these high Tl levels are associated to high Hg and As concentrations, as evidenced by the late-stage crystallization of complex Tl–Hg–As sulfosalts (Biagioni et al. 2014a, b). Though Tl minerals have been so far described for the Monte Arsiccio mine only, Tl has been also detected in the Sb-rich sterryite from the Pollone mine (Tl = 0.56 wt%; Moëlo et al. 2011). In addition, the occurrence of Hg sulfides and sulfosalts has been reported from Monte Arsiccio, Buca della Vena, and Pollone mines (e.g., Orlandi et al. 2007; Biagioni et al. 2013, 2014a, b, c). It is worthwhile to note that two relatively small Hg ore deposits occur very close to the study area and are hosted within the Paleozoic basement (Levigliani mine) and the Triassic quartzites/phyllites (Ripa mine; Dini et al., 2001). Based on the close field relationship between the Hg ores of Levigliani and the middle-late Ordovician calcalkaline metabasites occurring in the basement of the AA, Dini et al. (2001) proposed a genetic link between a Paleozoic Hg-metallogenetic event and coeval calcalkaline magmatism. The Hg ore deposit of Ripa is controlled by a late-Alpine shear zone propagating from the Paleozoic basement into the Triassic metamorphic cover (Dini et al. 2001).

Another striking geochemical signature of the pyrite ores from the studied area is represented by their lower As/Sb and Co/Ni ratios with respect to the pyrite ores from southern Tuscany. The Sb-rich nature of the orebodies from the AA is in keeping with the widespread occurrence of Pb–Sb sulfosalts in the hydrothermal veins from this area; in addition, Sb-analogues of As sulfosalts (e.g., boscardinite, the Tl-Sb homeotype of the As sulfosalt baumhauerite; Orlandi et al. 2012) have been described. High Ni contents are commonly observed in the ore deposits from the AA, as testified by the occurrence of several Ni sulfides in the orebodies or within late-stage Alpine veins (e.g., Benvenuti 1991).

Based on their Ag contents, the pyrite ores studied in this work, can be subdivided into two groups: an Ag-rich group (Monte Arsiccio, Buca della Vena, and Pollone mines), with an average Ag concentration of ~ 22 µg/g, and an Ag-poor group (Canale della Radice and Fornovolasco mines) with an average Ag concentration of ~ 1.8 µg/g. The Ag enrichment of the pyrite ores from the former group of ore deposits agrees with the occurrence of several Ag sulfosalts in late-stage Alpine extension veins in those localities (e.g., sterryite and associated Ag sulfosalts at the Pollone mine – Moëlo et al. 2011).

Finally, the V-enrichment of pyrite ores from AA is mirrored in the occurrence of V oxides (stibivanite, V-bearing derbylite, mannardite; Merlino and Orlandi 1983; Mellini et al. 1986; Biagioni et al. 2009) in extension veins. Additionally, V is a minor component of green mica and tourmaline occurring in Alpine veins from the Monte Arsiccio mine (authors' unpublished data).

The geochemistry of pyrite ores is thus reflected in the great variety of mineral species. Indeed, more than 270 different mineral species have been identified so far, with thirty-one species having their type-locality in AA. Among the latter, twenty-six have been found for the first time in the baryte – pyrite – iron oxide ore deposits, in several cases showing interesting crystal-chemical peculiarities related to the complex geochemistry of the ore deposits. It is worth noting that Tuscany is the most important Italian region for the occurrence and description of new mineral species, with 75 minerals having their type-locality there. It is impressive that 35% of them were described for the first time from the small baryte – pyrite – iron oxide mining district from southern AA. On the contrary, only few new mineral species were described from the larger iron and base metals deposits and the mercury and antimony mining districts from southern Tuscany. In fact, the former are well-known for museum-sized specimens of pyrite (as well as hematite, taking into account the iron ores from eastern Elba Island) but their mineral assemblages are usually formed by relatively common mineral species. The geochemical signature of pyrite ores from these districts are characterized by high Co (exceptionally up to 6020 µg/g in a sample from Rio Marina, in agreement with the occurrence of cobaltite described by Moresi and Quagliarella Asciano 1973) and high As contents. In some cases, Cu can be an important trace element (e.g., at the Monte Calamita mine), as well as Mn, particularly enriched in pyrite ores from the Campiglia Marittima skarn deposits, in keeping with the Mn-rich nature of their mineral association (e.g., the Ca-Mn clinopyroxene johannsenite, Mn-rich ilvaite, and the Cu-Mn sulfate mineral campigliaite; Vezzoni et al. 2016 and references therein). Generally, Sb occurs in very low amount; the scarcity of this element is reflected in the rarity of lead sulfosalts as well as stibnite from the iron and base metals orebodies from southern Tuscany.

The Hg-Sb mining district is usually characterized by a very simple mineralogy, with cinnabar and stibnite being the only ore minerals in the Hg and Sb mineralizations, respectively. Again, this is in contrast with the higher mineralogical-geochemical complexity of the AA district where the Hg ores host a larger variety of Hg-minerals (Dini et al. 2001). Iron sulfide samples from the mercury orebodies are usually characterized by high As/Sb ratios, with Sb usually occurring in extremely small amount, in agreement with the occurrence of trace amounts of orpiment and realgar as accessory minerals. An interesting feature is represented by Tl occurring in some samples; this element could reach concentrations (up to ≈ 250 μg/g) similar to those detected in some samples from AA. Exceptional Tl concentrations have been measured in a specimen of pyrite from the Tafone mine; it was the only available specimen of pyrite from the Sb mining district, so it could not be representative of the ore geochemistry of Sb deposits from southern Tuscany. It showed not only high Tl concentrations (the largest measured in this study) but also unusually high As as well as Sb contents. Unfortunately, few mineralogical as well as geochemical data are still available about the Sb deposits from southern Tuscany. The mineralogical studies have been usually focused on the secondary mineral assemblages, formed by Sb sulfates (e.g., peretaite, coquandite), whereas little is known about the possible occurrence of other accessory ore minerals. Indeed, such a high Tl content could suggest the possible occurrence of Tl minerals in the Tafone deposit.

Lead isotope data: regional variability and constraints on ore genesis

The limited variability of Pb-isotope compositions of pyrite, galena and sulfosalts from the southern AA (Table 4) indicates that Pb derived from a single source or from sources characterized by very similar U/Pb and Th/Pb ratios. More in detail, as already observed by Lattanzi et al. (1992), the slightly more radiogenic Pb isotope compositions of Monte Arsiccio and Fornovolasco ores could reflect the addition of Pb originating from *in situ* decay of Th and U. Indeed, complex uranium oxides (brannerite, dessauite(Y), mapiquiroite; Orlandi et al. 1997; Biagioni et al. 2014d) have been reported from these localities. The Pb-isotope compositions of the studied samples plot well above the two stage model of lead evolution curve of Stacey and Kramers (1975). In this respect they are similar to the Pb-isotope compositions of base-metal ores from southern Europe (e.g., García-Sansegundo et al. 2014). The Pb-isotope data for AA are in continuity with the general trend characterizing the ores generated during the Paleozoic metallogenetic event of Sardinia and its Variscan magmatic rocks (Fig. 7). This supports the similarities between the Paleozoic basement of Sardinia and that of the AA, as already

suggested on stratigraphic basis by several authors (e.g., Conti et al. 1993 and reference therein). It is worthwhile noting the gap of Pb-isotope compositions between the ores from AA and those from southern Tuscany. In the latter area the Pb-isotope signature of the ores is controlled by the Miocene to Pleistocene magmatism closely associated to the ore deposits (Fig. 7). Even though these magmas often are emplaced into a Paleozoic metasedimentary basement, the Pb-isotope signature of the ores excludes a significant contribution of Pb from the Paleozoic formations.

Lead-isotope data discard the early hypothesis of a genetic link between ores and a not yet identified Tertiary syntectonic magmatism at the roots of southern AA (Carmignani et al. 1972, 1976), and question the dubitative Quaternary age attribution of minor felsic bodies reported by Conti et al. (2010) in the same area.

Thallium-rich pyrite ore: new insights on the metallogeny of Apuan Alps

As briefly discussed above, the genesis of the ore deposits from AA has been debated by several authors. The deeper knowledge of the geochemistry of pyrite ores achieved during this study gives new insights on the metallogeny of this mining district. Indeed, the elemental association of Tl, Hg, Sb, and As characterizing these orebodies is known worldwide in two different kinds of hydrothermal deposits, i.e. stratiform basin-hosted sulfide deposits (e.g., Meggen, North-Rhine Westfalia, Germany; Krebs 1981) and Carlin-type deposits (e.g., Carlin, Nevada, USA; Radtke 1985).

Even if the current mineralogy, textures, and structural setting of the baryte – pyrite – iron oxide orebodies from southern AA are the result of a complex multistage evolution, some primary features can still be recognized: 1) their occurrence within the Paleozoic metasedimentary-metavolcanic sequence; 2) their association with tourmalinites; 3) their stratabound morphologies; 4) their mineralogical zoning, and, possibly, 5) their textural banding with alternating layers of baryte + pyrite (± tourmalinite) or baryte + iron oxides. These characteristics are more akin to those shown by stratiform basin-hosted sulfide deposits, whose main geological features are reviewed by Wilkinson (2014). This kind of hydrothermal deposits is characterized by stratiform and stratabound morphologies, with typical fine-grained layered and banded internal textures formed on or near the seafloor by precipitation from hydrothermal solutions. In addition, they are characterized by metal zoning of the ore bodies, from the inner/feeding zone towards the distal/discharging areas, with a progressive decrease of Cu, Zn, and Pb coupled with an increase of Ba and Mn (Galley et al. 2007; Wilkinson 2014). Hydrothermal activitiy is responsible for the formation of tourmalinites in many massive sulfide ore deposits (Palmer and Slack 1989).

The geochemistry of the stratiform basin-hosted sulfide deposits is related to the complex interplay between many factors, such as host-rock lithology, temperature of the hydrothermal fluids, and interaction between ore-forming fluids and sea water; usually, the primary geochemistry of these deposits is not significantly modified by later metamorphic and/or remobilization processes (e.g., Lengenbach, Switzerland, Hoffman and Knill 1996; Lanmuchang, China, Zhang et al. 2000).

The elemental association of Tl, Hg, As, and Sb (the so-called epithermal suite; Wilkinson 2014), characterizing the pyrite ores from southern AA, is a distinctive geochemical signature of low-temperature hydrothermal systems (*T* generally below 300 °C), in some cases associated with a coeval felsic magmatism. Moreover, a genesis from fluids derived from an evolved continental crust within intracontinental marine basins is typical of this elemental association (Leach et al. 2005; Wilkinson 2014). Data on active sea-floor hydrothermal systems agree with this interpretation, showing orebodies associated with transitional arcs and intracontinental back-arc basin richer in Hg, As, Sb, as well as Tl, than those occurring at mid-ocean ridges, ridge-hot spot intersections, and intraoceanic back-arc basins (Hannington et al. 2005; Wilkinson 2014). In addition, the geochemistry of the vent fluids discharged in intracontinental settings records higher concentrations of Zn, Pb, Ag, As, Sb, Hg, Ba, and Au with respect to the typical Cu, Fe, Co, Se, and Ni association characterizing intraoceanic settings. The low Co/Ni ratio shown by the pyrite ores from southern AA supports the hypothesis of an intracontinental back-arc basin or a transitional arc setting for the genesis of the orebodies (Hannington et al. 2005, and references therein). Accordingly, the geochemistry of the baryte – pyrite – iron oxide ore deposits of AA coupled with their geological setting agree with an origin as stratiform basin-hosted sulfide deposits in an intracontinental setting. The enrichment in V and Mo could be interpreted as the result of a possible interaction between orebodies and sea-water (e.g., Hoffman and Knill 1996).

In this scenario, the timing of ore genesis of the baryte – pyrite – iron oxide orebodies could be dated to the early Paleozoic, coeval with the genesis of the Pb-Ag-Zn proto-ores of the Bottino mine, the formation of tourmalinite, and the felsic magmatism. As a matter of fact, several authors suggest a Paleozoic origin of tourmalinite (Benvenuti et al. 1989; Lattanzi et al. 1994; Pandeli et al. 2004) and its pre-Ladinian origin could be supported by the regional occurrence of tourmalinite clasts with the Verrucano formation (e.g., Rau and Tongiorgi 1974; Cavarretta et al. 1992). Finally, lead-isotope data of pyrite ores, and associated Pb-Zn-Ag ores, support this hypothesis.

Taking as a whole, the mining district of southern AA shows the elemental association of Pb, Zn, Cu, Sb, As, Tl, Hg, Ba, and Fe with a continuous transition from Bottino type (Pb, Zn, Ag, Cu) ore towards baryte –

pyrite – iron oxide ores. The different mineralogy and geochemistry between these two kinds of ore deposits could reflect an original zoning in the stratiform basin-hosted sulfide deposit, with the Pb-Zn-Ag-Cu ores formed close to the feeding vents and the baryte – pyrite – iron oxide ores occurring in distal areas. Further field and laboratory investigations are needed to confirm this hypothesis.

Thallium-rich pyrite ores, acid mine drainage, and environmental hazard

The finding of high Tl concentrations in pyrite ores from southern AA poses some concerns related to the potential dispersion of this element in the environment following pyrite oxidation and the formation of acid mine drainage systems. Indeed, the high rainfall characterizing the areas hosting the Tl-bearing mineralization (more than 3000 mm/a; Giannecchini 2006), as well as the occurrence of permeable to highly permeable lithologies favoring a pervasive groundwater circulation, expose the pyrite ore bodies to oxidation. Therefore, the release and dispersion of potentially toxic elements, including Tl, and the production of AMD is enhanced (Fig. 10a, b). Preliminary hydrogeochemical data show that the strongly acidic (pH = 1.1-2.4) internal waters of Monte Arsiccio, Pollone and Canale della Radice mines have extremely high concentrations of Tl (commonly ~ 1000 µg/l and up to 9000 µg/l; authors' unpublished data), clearly indicating the passage of Tl from the pyrite ores into the aqueous phase. The steps involved in the process of pyrite oxidation and release of its metal content are currently under study and are mainly focused on the mineralogy and geochemistry of the many Fe sulfates (e.g., Biagioni et al. 2011) occurring in association with pyrite. The occurrence of colonies of iron-oxidizing bacteria forming abundant slime-like masses inside the abandoned tunnels (Fig. 10c) indicates that the production of AMD from these mines is enhanced by biotic processes.

The most severe contamination affects the village of Valdicastello Carducci and the town of Pietrasanta (Lucca Province), owing to the continuous drainage of mine waters from the Monte Arsiccio and Pollone abandoned mines into the Baccatoio stream (Fig. 10a, b). At the beginning of September 2014 researchers of the Pisa University's Dipartimento di Scienze della Terra, including one of the authors of this paper (MDO), reported to the local authorities the presence of thallium in concentrations up to 10.1 µg/l in the water of the public water supply system feeding the Valdicastello Carducci village, exposing about 1000 residents to this heavy element (Campanella et al. 2016). The source of contamination was soon identified in a water spring (Molini di Sant'Anna) located within the mineralized area between the Monte Arsiccio and Pollone mines. The water collected from this spring fed part of the water supply system of Valdicastello Carducci and Pietrasanta

and, immediately after the report of the Tl contamination, it was excluded from the system. It is worthwhile noting that in terms of its inorganic chemical components, the water emerging from the Molini di Sant'Anna spring is of good quality with the notable exception of Tl, and sometimes Fe and Mn. This observation emphasizes the peculiar aqueous geochemistry of Tl, which should be dominantly present in solution as Tl^+ over a large interval of pH and Eh conditions (e.g., Xiong 2007). At moderately low concentrations (up to hundreds of µg/l) Tl is a very mobile element that can not be removed from water by precipitation because no insoluble solid phases form at pH and Eh conditions commonly occurring in natural environments.

At a regional scale, the geochemistry of pyrite ores from the other mining districts indicate that it is unlikely that similar Tl pollution could occur in other areas of Tuscany, with the notable exception of the Sb-Hg districts. In fact, as noted above, some samples show high Tl contents and consequently this mining district should deserve further investigations in order to rule out the possible Tl dispersion into the environment.

Conclusions

The following conclusions can be drawn based on our geochemical study of the pyrite ores from the AA and southern Tuscany:

- The pyrite ores from the baryte – pyrite – iron oxide orebodies occurring in the southern portion of the AA are characterized by a significant Tl content (always > 10 µg/g, commonly > 100 µg/g, and up to 1100 µg/g). High Tl concentrations are associated to high As and Sb levels, and, to minor extent, V, Mo and Ni. The actual speciation of Tl, As, and Sb within these pyrite ores should be further investigated through a multi-technique approach, coupling data resulting from LA-ICP-MS, TEM, and XAS experiments.
- Pyrite ores from the Fe and base metal orebodies of southern Tuscany (including Elba and Giglio islands) have low to very low concentrations of Tl (mostly < 0.5 µg/g and up to 2 µg/g). In addition to their much higher content of Tl, the pyrite ores from southern AA strongly differ from those of the Fe and base metal orebodies of southern Tuscany for their much lower Co/Ni and As/Sb ratios, higher Mo and V contents, and less radiogenic Pb isotope composition. These differences suggest a markedly different origin and geologic evolution of the pyrite ores from these mining districts.
- Data on the pyrite/marcasite ores associated to the Hg – Sb ore deposits from southern Tuscany are too scarce and variable to draw some generalizations; however, some occurrences (e.g., Siele, Pietrineri and Tafone

mines) show evidences of high to extremely high Tl contents (up to ~ 3900 µg/g in one sample from Tafone mine).

- The Pb isotope composition of sulfides and sulfosalts from southern AA, the typical association of these orebodies with tourmalinites and the close relationship of several orebodies with early Paleozoic igneous rocks (metarhyolite) suggest that the proto-ores of these deposits formed during early Paleozoic and were later reworked during the Apennine orogeny and, possibly the Variscan orogeny.
- Knowledge of the geochemistry of pyrite ores from AA and southern Tuscany is fundamental for assessing the impact of ore deposits on the environment and for the management of the environmental concerns. In particular, the finding of the high Tl content of pyrite ores from AA allowed the discovery of the severe Tl pollution of drinkable water in the municipality of Pietrasanta (Lucca Province), stressing the important social, as well as economic, impact of geochemistry.

Acknowledgments

This research received support by Ministero dell'Istruzione, dell'Università e della Ricerca through the project SIR 2014 "THALMIGEN – Thallium: Mineralogy, Geochemistry, and Environmental Hazards", granted to CB. We are grateful to Davide Franceschelli and Simone Beccari (Museo delle Miniere di Mercurio del Monte Amiata, Santa Fiora, Grosseto, Italy) for providing us with some specimens of pyrite/marcasite from the Monte Amiata Hg district. The paper benefited from the constructive criticism of the two reviewers Artur Deditius and Kalin Kouzmanov and the Editor-in-chief Bernd Lehmann.

References

Batley GE, Florence TM (1975) Determination of thallium in natural waters by anodic stripping voltammetry. J Electroanal Chem 61:205-211

Benvenuti M (1991) Ni-sulphides from the Bottino mine (Tuscany, Italy). Eur J Mineral 3:79-84

Benvenuti M, Lattanzi P, Tanelli G, Cortecci G (1986) The Ba-Fe-pyrite deposit of Buca della Vena, Apuan Alps, Italy. Rend Soc Ital Mineral Petrol 41:347-358

Benvenuti M, Lattanzi P, Tanelli G (1989) Tourmalinite-associated Pb-Zn-Ag mineralization at Bottino, Apuan Alps, Italy: geologic setting, mineral textures, and sulfide chemistry. Econ Geol 84:1277-1292

Benvenuti M, Tanelli G, Cortecci G, Lattanzi P (1990) Geology, mineralogy and geochemistry of the barite-pyrite (Pb-Ag) deposit at Pollone, Apuane Alps. Boll Soc Geol Ital 109:735-741

Bergmann H (1969) Geologische und lagerstättenkundliche untersuchugen in den südwestlichen Apuaner Alpen (Toskana, Italien). Ph.D. Thesis, Ludwig-Maximilians-Universität München

Biagioni C, Orlandi P, Pasero M (2009) Ankangite from the Monte Arsiccio mine (Apuan Alps, Tuscany, Italy): occurrence, crystal structure, and classification problems in cryptomelane group minerals. Period Mineral 78:3-11

Biagioni C, Bonaccorsi E, Orlandi P (2011) Volaschioite, $Fe^{3+}{}_4(SO_4)O_2(OH)_6{\cdot}2H_2O$, a new mineral species from Fornovolasco, Apuan Alps, Tuscany, Italy. Can Mineral 49:605-614

Biagioni C, D'Orazio M, Vezzoni S, Dini A, Orlandi P (2013) Mobilization of Tl-Hg-As-Sb-(Ag,Cu)-Pb sulfosalt melts during low-grade metamorphism in the Alpi Apuane (Tuscany, Italy). Geology 41:747-750

Biagioni C, Bonaccorsi E, Moëlo Y, Orlandi P (2014a) Mercury-arsenic sulfosalts from the Apuan Alps (Tuscany, Italy). I. Routhierite, $(Cu_{0.8}Ag_{0.2})Hg_2Tl(As_{1.4}Sb_{0.6})_{\Sigma=2}S_6$, from Monte Arsiccio mine: occurrence and crystal structure. Eur J Mineral 26:163-170

Biagioni C, Bonaccorsi E, Moëlo Y, Orlandi P, Bindi L, D'Orazio M, Vezzoni S (2014b) Mercury-arsenic sulfosalts from the Apuan Alps (Tuscany, Italy). II. Arsiccioite, $AgHg_2TlAs_2S_6$, a new mineral from the Monte Arsiccio mine: occurrence, crystal structure and crystal chemistry of the routhierite isotypic series. Mineral Mag 78:101-117

Biagioni C, Moëlo Y, Orlandi P (2014c) Lead-antimony sulfosalts from Tuscany (Italy). XV. (Tl-Ag)-bearing rouxelite from Monte Arsiccio mine: occurrence and crystal chemistry. Mineral Mag 78:651-661

Biagioni C, Orlandi P, Pasero M, Nestola F, Bindi L (2014d) Mapiquiroite, $(Sr,Pb)(U,Y)Fe_2(Ti,Fe^{3+})_{18}O_{38}$, a new

member of the crichtonite group from the Apuan Alps, Tuscany, Italy. Eur J Mineral 26:427-437

Biagioni C, Dini A, Orlandi P, Moëlo Y, Pasero M, Zaccarini F (2016) Lead-antimony sulfosalts from Tuscany (Italy). XX. Members of the jordanite–geocronite series from the Pollone mine, Valdicastello Carducci: occurrence and crystal structures. Minerals 6, doi:10.3390/min6010015

Boni M, Koeppel V (1985) Ore-lead isotope pattern from the Iglesiente-Sulcis Area (SW Sardinia) and the problem of remobilization of metals. Mineral Deposita 20:185-193

Boni M, Iannace A, Koeppel V, Früh-Green G, Hansmann W (1992) Late to post-hercynian hydrothermal activity and mineralization in southwest Sardinia (Italy). Econ Geol 87:2114-2137

Campanella B, Onor M, D'Ulivo A, Giannecchini R, D'Orazio M, Petrini R, Bramanti E (2016) Human exposure to thallium through tap water: A study from Valdicastello Carducci and Pietrasanta (northern Tuscany, Italy). Sci Total Environ 548-549: 33-42

Carmignani L, Dessau G, Duchi G (1972) I giacimenti minerari delle Alpi Apuane e loro correlazioni con l'evoluzione del gruppo montuoso. Mem Soc Geol Ital 11:417-431

Carmignani L, Dessau G, Duchi G (1975) Una mineralizzazione sin-tettonica: il giacimento di Valdicastello (Alpi Apuane). Rapporti fra tettonica e minerogenesi in Toscana. Boll Soc Geol Ital 94:725-758

Carmignani L, Dessau G, Duchi G (1976) I giacimenti a barite, pirite ed ossidi di ferro delle Alpi Apuane. Studio minerogenetico e strutturale. Boll Soc Geol Ital 95:1009-1061

Cavarretta G, Franceschelli M, Pandeli E, Puxeddu M, Valori A (1992) Tourmalinites from the Triassic Verrucano of the Northern Apennines, Italy. Newsletter-International Union of Geological Sciences, Commission on Stratigraphy, Subcommission on Devonian Stratigraphy, 5:335-338

Chappaz A, Lyons TW, Gregory DD, Reinhard CT, Gill BC, Li C, Large RR (2014) Does pyrite act as an important host for molybdenum in modern and ancient euxinic sediments? Geochem Cosmochem Acta 126:112-122

Ciarapica G, Olivero S, Passeri L (1985) Inquadramento geologico delle principali mineralizzazioni apuane ed indizi a favore di una metallogenesi triassica. Industria Mineraria 1:19-37

Conti P, Di Pisa A, Gattiglio M, Meccheri M (1993) The pre-Alpine basement in the Alpi Apuane (Northern Apennines, Italy). In: Von Raumer JF, Neubauer F (eds) Pre-Mesozoic Geology in the Alps. Springer-Verlag, Berlin, pp 609-621

Conti P, Massa G, Meccheri M, Carmignani L (2010) Geological map of the Stazzema area (Alpi Apuane, Northern Apennines, Italy). Scale 1/10000. Centro di Geotecnologie, Università di Siena

Cortecci G, Lattanzi P, Tanelli G (1985) Barite-iron oxides-pyrite deposits from Apuane Alps, northern Tuscany, Italy. Mem Soc Geol Ital 30:337-345

Cortecci G, Benvenuti M, Lattanzi P, Tanelli G (1992) Stable isotope geochemistry of carbonates from the Apuane Alps mining district, northern Tuscany, Italy. Eur J Mineral 4:509-520

Costagliola P, Benvenuti M, Tanelli G, Cortecci G, Lattanzi P (1990) The barite-pyrite-iron oxides deposit of Monte Arsiccio (Apuane Alps): geological setting, mineralogy, fluid inclusions, stable isotope and genesis. Boll Soc Geol Ital 109:267-277

Costagliola P, Benvenuti M, Lattanzi P, Tanelli G (1998) Metamorphogenic barite-pyrite (Pb-Zn-Ag) veins at Pollone, Apuane Alps, Tuscany: vein geometry, geothermobarometry, fluid inclusions and geochemistry. Mineral Petrol 62:29-60

Craig JR, Vokes FM (1993) The metamorphism of pyrite and pyritic ores: an overview. Mineral Mag 57:3-18

Deditius AP, Utsunomiya S, Renock D, Ewing RC, Ramana CV, Becker U, Kesler SE (2008) A proposed new type of arsenian pyrite: Composition, nanostructure and geological significance. Geochem Cosmochem Acta 72:2919-2933

Deditius AP, Utsunomiya S, Kesler SE, Reich M, Ewing RC (2011) Trace elements nanoparticles in pyrite. Ore Geol Rev 42:32-46

Deditius AP, Reich M (2016) Constraints on the solid solubility of Hg, Tl and Cd in arsenian pyrite. Am Min 101:1451-1459

Dini A (2003) Ore deposits, industrial minerals and geothermal resources. In: Poli G et alii (eds) Miocene to Present Plutonism and Volcanism in the Tuscan Magmatic Province (Central Italy). Period Mineral Spec Issue 72:41-52

Dini A, Benvenuti M, Costagliola P, Lattanzi P (2001) Mercury deposits in metamorphic settings: the example of Levigliani and Ripa mines, Apuane Alps (Tuscany, Italy). Ore Geol Review 18:149-167

Dini A, Di Vincenzo G, Ruggieri G, Rayner J, Lattanzi PF (2005) Monte Ollasteddu, a new gold discovery in the Variscan basement of Sardinia (Italy): first isotopic (^{40}Ar-^{39}Ar, Pb) and fluid inclusion data. Mineral Deposita 40:337-346

Fellin MG, Reiners PW, Brandon MT, Wüthrich E, Balestrieri ML, Molli G (2007) Thermochronologic evidence for exhumational history of the Alpi Apuane metamorphic core complex, northern Apennines, Italy. Tectonics 26, doi:10.1029/2006TC002085

Galley AG, Hannington M, Jonasson I (2007) Volcanogenic massive sulphide deposits. In: Goodfellow WD (ed) Mineral deposits of Canada: a synthesis of major deposit-types, district metallogeny, the evolution of geological provinces, and exploration methods. Geol Ass Canada Mineral Dep Div, Spec Publ 5:141-161

García-Sansegundo J, Martin-Izard A, Gavaldà J (2014) Structural control and geological significance of the Pb-Zn ores formed in the Benasque Pass area (Central Pyrenees) during the post-late Ordovician extensional event of the Gondwana margin. Ore Geol Review 56:516-527

Giannecchini R (2006) Relationship between rainfall and shallow landslides in the southern Apuan Alps (Italy). Nat Hazards Earth Syst Sci 186:357-364

Hannington MD, de Ronde CEJ, Petersen S (2005) Sea-floor tectonics and submarine hydrothermal systems. Econ Geol 100:111-141

Hein JR, Koschinsky A, Bau M, Manheim FT, Kang J-K, Roberts L (2000) Cobalt-rich ferromanganese crusts in the Pacific. In: Cronan DS (ed) Handbook of Marine Mineral Deposits. CRC Press, Boca Raton, pp 239-279

Hoffman BA, Knill MD (1996) Geochemistry and genesis of the Lengenbach Pb-Zn-As-Tl-Ba mineralization, Binn Valley, Switzerland. Mineral Deposita 31:319-339

Huston DL, Sie SH, Suter GF, Cooke DR, Both RA (1995) Trace elements in sulfide minerals from eastern Australian volcanic-hosted massive sulfide deposits; Part I, Proton microprobe analyses of pyrite, chalcopyrite, and sphalerite, and Part II Selenium levels in pyrite; comparison with delta ^{34}S values and implications for the source of sulfur in volcanogenic hydrothermal systems. Econ Geol 90:1167-1196

Hsu LC, Galli PE (1973) Origin of the scheelite-powellite series of minerals. Econ Geol 68:681-696

Iskowitz JM, Lee JJH, Zeitlin H (1982) Determination of thallium in deep-sea ferromanganese nodules. Marine Mining 3:285-295

Karlsson U, Karlsson S, Düker A (2006) The effect of light and iron(II)/iron(III) on the distribution of Tl(I)/Tl(III) in fresh water systems. J Environ Monit 8:634-640

Krebs W (1981) The geology of the Meggen ore deposit. In: Wolf KH (ed) Handbook of Stratiform and Stratabound Ore Deposits, vol 9. Elsevier, Amsterdam, pp 509-549

Krupp RE, Seward TM (1990) Transport and deposition of metals in the Rotokawa geothermal system, New Zealand. Mineral Deposita 25:73-81

Lattanzi P, Hansmann W, Koeppel V, Costagliola P (1992) Source of metals in metamorphic ore-forming processes in the Apuane Alps (NW Tuscany, Italy): constraints by Pb-isotope data. Mineral Petrol 45:217-229

Lattanzi P, Benvenuti M, Costagliola P, Tanelli G (1994) An overview on recent research on the metallogeny of Tuscany, with special reference to the Apuane Alps. Mem Soc Geol Ital 48:613-625

Lattanzi P, Benvenuti M, Gale N, Hansmann W, Koeppel V, Stos-Gale Z (1997) Pb isotopes data on ore deposits of southern Tuscany. Proceedings of the 1st "F.I.S.T." Congress, 5-9 October 1997, Bellaria, 123-124

Leach DL, Sangster DF, Kelley KD, Large RR, Garven G, Allen CR, Gutzmer J, Walters S (2005) Sediment-hosted lead-zinc deposits: A global perspective. Econ Geol 100:561-607

Ludwig KR, Vollmer R, Turi B, Simmons KR, Perna G (1989) Isotopic constraints on the genesis of base-metal ores in southern and central Sardinia. Eur J Mineral 1:657-666

Lustrino M, Duggen S, Rosenberg CL (2011) The Central-Western Mediterranean: anomalous igneous activity in an anomalous collisional tectonic setting. Earth Sci Rev 104:1-40

Mellini M, Orlandi P, Vezzalini G (1986) V-bearing derbylite from the Buca della Vena mine, Apuan Alps, Italy. Mineral Mag 50:328-331

Merlino S, Orlandi P (1983) A second occurrence of stibivanite: Buca della Vena mine (Apuan Alps), Italy. Can Mineral 21:159-160

Moëlo Y, Orlandi P, Guillot-Deudon C, Biagioni C, Paar W, Evain M (2011) Lead-antimony sulfosalts from Tuscany (Italy). XI. The new mineral species parasterryite, $Ag_4Pb_{20}(Sb_{14.5}As_{9.5})_{\Sigma 24}S_{58}$, and associated sterryite, $Cu(Ag,Cu)_3Pb_{19}(Sb,As)_{22}(As–As)S_{56}$, from the Pollone mine, Tuscany, Italy. Can Mineral 49:623-638

Moresi M, Quagliarella Asciano F (1973) Cobaltite negli skarn della Torre di Rio (Isola d'Elba). Period Mineral 42:173-182

Natale P (1974) Relitti di bassa temperatura nelle piriti di alcuni giacimenti della Toscana. Boll Assoc Miner Sudalpina, Anno XI, 1-2:1-21

Nriagu JO (1998) History, production and uses of thallium. In: Nriagu JO (ed) Thallium in the Environment. Wiley-Interscience, London, pp 1-14

Orberger B, Arnold M, Saupé F (1986) Sulfur isotopic studies of the minerals from the Pollone and Monte Arsiccio deposits (SW Apuane Alps, Tuscany, Italy). Contribution to the knowledge of the ore deposits of Tuscany, III. Fortschr Mineral 64:215-226

Orlandi P, Pasero M, Duchi G, Olmi F (1997) Dessauite, (Sr,Pb)(Y,U)(Ti,Fe^{3+})$_{18}O_{38}$, a new mineral of the crichtonite group from Buca della Vena mine, Tuscany, Italy. Am Mineral 82:807-811

Orlandi P, Moëlo Y, Campostrini I, Meerschaut A (2007) Lead-antimony sulfosalts from Tuscany (Italy). IX. Marrucciite, $Hg_3Pb_{16}Sb_{18}S_{46}$, a new sulfosalt from Buca della Vena mine, Apuan Alps: definition and crystal structure. Eur J Mineral 19:267-279

Orlandi P, Biagioni C, Bonaccorsi E, Moëlo Y, Paar WH (2012) Lead-antimony sulfosalts from Tuscany (Italy). XII. Boscardinite, $TlPb_4(Sb_7As_2)_{\Sigma 9}S_{18}$, a new mineral species from the Monte Arsiccio mine: occurrence and crystal structure. Can Mineral 50:235-251

Orlandi P, Biagioni C, Moëlo Y, Bonaccorsi E, Paar WH (2013) Lead-antimony sulfosalts from Tuscany (Italy). XIII. Protochabournéite, ~$TlPb_2(Sb_{9-8}As_{1-2})_{\Sigma 10}S_{17}$, from the Monte Arsiccio mine: occurrence, crystal structure and relationship with chabournéite. Can Mineral 51:475-494

Palmer MR, Slack JF (1989) Boron isotopic composition of tourmalines from massive sulfide deposits and tourmalinites. Contrib Mineral Petrol 103:434-451

Pandeli E, Bagnoli P, Negri M (2004) The Fornovolasco schists of the Apuan Alps (Northern Tuscany, Italy): a new hypothesis for their stratigraphic setting. Boll Soc Geol Ital 123:53-66

Peter ALJ, Viraraghavan T (2005) Thallium: a review of public health and environmental concerns. Environ Int 31:439-501

Radtke AS (1985) Geology of the Carlin gold deposit, Nevada, USA. U.S. Geological Survey Professional Paper 1267:241-246

Ralph L, Twiss MR (2002) Comparative toxicity of thallium(I), thallium(III) and cadmium(II) to the unicellular alga *Chlorella* isolated from Lake Erie. Bull Environ Contam Toxicol 68:261-268

Rau A., Tongiorgi M. (1974) Geologia dei Monti Pisani a sud-est della Valle del Guappero. Mem Soc Geol It 13:227-408

Rehkämper M, Frank M, Hein JR, Halliday A (2004) Cenozoic marine geochemistry of thallium deduced from isotopic studies of ferromanganese crusts and pelagic sediments. Earth Planet Sci Lett 219:77-91

Rimondi V, Chiarantini L, Lattanzi P, Benvenuti M, Beutel M, Colica A, Costagliola P, Di Benedetto F, Gabbani G, Gray J, Pandeli E, Pattelli G, Paolieri M, Ruggieri G (2015) Metallogeny, exploitation and environmental impact of the Mt. Amiata mercury ore district (Southern Tuscany, Italy). Ital J Geosci 134:323-336

Shannon RD (1976) Revised effective ionic radii and systematic studies of interatomic distances in halides and chalcogenides. Acta Crystallogr A32:751-767

Stacey JS, Kramers JD (1975) Approximation of terrestrial lead isotope evolution by a two-stage model. Earth Planet Sci Lett 26:207-221

Stos–Gale Z, Gale NH, Houghton J, Speakman R (1995) Lead isotopes from Isotrace Laboratory, Oxford: Archaeometry database 1, ores from western Mediterranean. Archaeometry 37:407-415

Tanelli G, Benvenuti M, Costagliola P, Dini A, Lattanzi P, Maineri C, Mascaro I, Ruggieri G (2001). The iron mineral deposits of Elba Island: state of the art. Ofioliti 26:239-248

Todt W, Cliff RA, Hanser A, Hofmann AW (1993) Recalibration of NBS lead standards using a ^{202}Pb–^{205}Pb double spike. Terra Abstr 5:396

Vezzoni S, Dini A, Rocchi S (2016) Reverse telescoping in a distal skarn system (Campiglia Marittima, Italy). Ore Geol Rev 77:176-193

Vorlicek TP, Kahn MD, Kasuya Y, Helz GR (2004) Capture of molybdenum in pyrite-forming sediments: Role of ligand-induced reduction by polysulfides. Geochem Cosmochem Acta 68:547-556

Wedepohl KH (1995) The composition of the continental crust. Geochim Cosmochim Acta 59:1217-1239

Wilkinson JJ (2014) Sediment-hosted zinc-lead mineralization: Processes and perspectives, In: Holland HD, Turekian KK (eds) Geochemistry of Mineral Deposits. Elsevier, Oxford, pp 219-249

Xiong Y (2007) Hydrothermal thallium mineralization up to 300 °C: a thermodynamic approach. Ore Geol Rev 32:291-313

Zhang Z, Zhang B, Chen Y., Zhang X (2000) The Lanmuchang Tl deposit and its environmental geochemistry. Science in China (Series D) 43: 50-62

Zhou TF, Fan Y, Yuan F, Wu MA, Hou MJ, Voicu G, Hu QH, Zhang QM, Yue SC (2005) A preliminary geological and geochemical study of the Xiangquan thallium deposit, eastern China: the world's first thallium-only mine. Mineral Petrol 85:243-251

Table captions

Table 1 Details of the pyrite/marcasite ores from Tuscany analyzed in this study

Table 2 Analyzed isotopes, operation mode, and detection limits (µg/g in the solid sample) for the ICP-MS analyses

Table 3 Trace-element analyses of pyrite ores from the southern Apuan Alps. Concentrations in µg/g

Table 4 Lead isotope compositions of pyrite ores and lead sulfides and sulfosalts from the southern Apuan Alps

Table 5 Trace-element analyses of pyrite/marcasite ores from southern Tuscany. Concentrations in µg/g

Figure captions

Fig. 1 Sketch maps showing the localities cited in the text

Fig. 2 Simplified geological map of the southern Apuan Alps. Abandoned mines: 1, Pollone; 2, Monte Arsiccio; 3, Canale della Radice; 4, Buca della Vena; 5, Fornovolasco; 6, Argentiera di Sant'Anna; 7, La Tana; 8, Buca dell'Angina; 9, Bottino; 10, Levigliani

Fig. 3 Country rocks and orebodies from the baryte – pyrite – iron oxide abandoned mines of the southern Apuan Alps. (a) Lensoidal microgranular pyrite orebody (Canale della Radice mine); (b) outcrop of pyrite-bearing schist near the Fornovolasco mine; (c) tourmalinite layers embedded within schist at the footwall of the Monte Arsiccio mine; (d) banded and folded pyrite + baryte ore, surficially altered into blue-greenish melanterite (Pollone mine)

Fig. 4 Macroscopic thallium sulfosalts from the Monte Arsiccio mine. (a) Routhierite filling small cracks within pyrite-bearing metadolostone; (b) protochabournéite + stibnite within pyrite-bearing metadolostone; (c) elongated mass of protochabournéite within granular baryte + pyrite ore; (d) protochabournéite + arsiccioite within granular baryte + pyrite ore

Fig. 5 a, b, c, d, e, f) Back-scattered electron images of pyrite ores from the southern Apuan Alps showing variable textures and mineral assemblages. Sample labels as in Table 1. Abbreviations: Ap, apatite; Apy, arsenopyrite; Brt, baryte; Cal, calcite; Chl, chlorite; Dol, dolomite; Gn, galena; Ms, muscovite, Py, pyrite; Qtz, quartz; Sd, siderite. Boscardinite is a Tl-Pb-Sb-As sulfosalt, $TlPb_4(Sb_7As_2)S_{18}$, first discovered in the Monte Arsiccio mine (Orlandi et al. 2012)

Fig. 6 Plots of Sb (a), As (b), V (c), and Mo (d) vs Tl for the southern Apuan Alps pyrite ores. Logarithmic scale

Fig. 7 $^{208}Pb/^{204}Pb$ (a) and $^{207}Pb/^{204}Pb$ (b) vs $^{206}Pb/^{204}Pb$ for pyrite, galena and lead sulfosalts from the southern Apuan Alps (1) compared to Miocene-Pleistocene ores (2) and magmatic rocks (3) from southern Tuscany, and

Paleozoic ores (4) and Variscan magmatic rocks (5) from Sardinia. The insets show the data from this study with different symbols for different ore type. Data sources: Apuan Alps: this study, Lattanzi et al. (1992); Sardinia: Boni and Koeppel (1985), Ludwig et al. (1989), Boni et al. (1992), Dini et al. (2005); southern Tuscany: Stos-Gale et al. (1995), Lattanzi et al. (1997), Lustrino et al. (2011) and references therein. The two-stage Pb isotope evolution curve of Stacey and Kramers (1975) is also plotted for reference

Fig. 8 Plots of Co/Ni (a), As/Sb (b) and V (c) vs Tl for the pyrite ores from Tuscany. Symbols: white circles, southern Tuscany Fe and base metals deposits; crosses, southern Tuscany Hg and Sb deposits; same symbols of Figure 6, Apuan Alps pyrite ores

Fig. 9 Plot of molar concentration of (Sb+As) vs molar concentration of (Tl+Cu+Ag) for the southern Apuan Alps pyrite ores. In the diagram are also plotted the displacement vector for the substitution 2 Fe^{2+} = $(Tl,Cu,Ag)^{+}$ + $(As,Sb)^{3+}$ within the pyrite lattice, and the displacement vector for the addition of arsenopyrite and/or stibnite to the pyrite ores and for the substitution $(S_2)^{2-}$ = $[(As,Sb)S]^{2-}$ within the pyrite latttice. Same symbols of Figure 6

Fig. 10 a, b) The heavily polluted water of the Baccatoio stream flowing across the Monte Arsiccio mining area. c) Stalactite-like biofilm structures produced by iron-oxidizing bacteria and other microbic living organisms. The yellow matter close to the biofilm is Tl-bearing jarosite (Monte Arsiccio mine)

UNIVERSITÀ DI PISA
DIPARTIMENTO DI SCIENZE DELLA TERRA

October 12, 2016

Manuscript

Dear Prof. Lehmann,

we have taken into account the comments and the corrections suggested by the two reviewers, modifying the manuscript in agreement with their suggestions. In the following, you will find the detailed replies to the main questions raised by the reviewers (and also by you, as concern the absence of any gold data).

Yours sincerely,

Cristian Biagioni

Via Santa Maria, 53 · 56126 Pisa · Italia
tel. (+39) 050 2215 700 · fax (+39) 050 2215 800 · sito web: www.dst.unipi.it
cod. fiscale 80003670504 · partita IVA 00286820501

Reviewer #1 (Kalin Kouzmanov)
We are grateful to the reviewer for his constructive suggestions and criticisms. All his corrections have been taken into account and added to the revised version of the manuscript. The following questions have to be addressed.

R: Table 1 could be enlarged in order to include more information about the mineral composition of the samples studied – useful for the interpretation of the trace element data.

We prefer to add more details in the text, adding a description of the mineral assemblages of the pyrite ores studied in the Results section.

R: Presence of particular mineral inclusions, their size, abundance, location in the pyrite etc. should be reported to help the discussion.

The manuscript has been improved adding a description of the mineralogy of the pyrite ores. As reported in Table 1, pyrite ores from Apuan Alps are mainly composed by pyrite. Some information about the accessory minerals has been added. In addition, the geochemistry of the pyrite ores from Apuan Alps is discussed taking into account their mineralogical composition (see the new paragraph "Relationships between geochemistry and mineralogy of pyrite ores from the southern Apuan Alps").

R: Information about how the 50 mg of sample used for the ICP-MS analyses was separated is also missing – in situ sampling (micro-drilling) versus bulk sampling (homogenization of the sample) could have an important impact on the interpretation of the results.

The text has been modified adding a brief description of the sample preparation.

R: Correlations between Tl and other trace elements or element ratios have been discussed, but no correlations between other mono, di- or trivalent elements.

The relationships between these elements have been discussed in the text.

R: Is there any particular reason why elements such as Au, Hg, Se, Te, Bi have not been analyzed? One of the questions discussed in the paper is the environmental impact during oxidation of such pyrite ores, but the content of other "toxic" elements like Hg, Te were not reported to complete the data on Tl and As.

We agree that these elements are important for geochemical systems such as those studied in our work. However, there are major analytical problems in determining these elements in our laboratory. Mercury, Au, Se, and Te have very high first ionization potentials and hence are not very efficiently ionized in the Argon plasma of ICP-MS spectrometer. This is particularly true for Hg. In addition this latter element is partially volatilized during the acid dissolution of pyrite ore samples. The sensitivity for Au would be sufficiently high but the low concentrations expected would impose a low dilution of the samples and this in turn will cause a severe contamination of the spectrometer in Tl, Fe, As, and other elements. In other words, the determination of these elements requires specific analytical methods (e.g. preconcentration methods for Au analysis, cold vapour

for Hg) that have not yet been developed in our lab. Unfortunately modern literature data for these elements in the pyrite ore of Tuscany are not available.

R: "Most probably from magnetite impurities in the samples analyzed".

Magnetite was usually not observed in pyrite ores (it occurs only as accessory mineral in some samples from Buca della Vena mine), whereas V could be hosted in light-green flakes of mica observed as interstitial minerals in some samples (in particular in V-rich samples from Canale della Radice).

R: In the discussion the authors defend the hypothesis that all trace elements in the analyzed pyrites from this study are due to minor solid inclusions of other sulfide and sulfosalt minerals. Here is no discrimination between trace elements in the pyrite structure and elements due to solid inclusions. However, number of the analyzed trace elements could potentially be fixed in the pyrite structure – As, Co, Ni, Sb.

Actually, in our discussion, we compare the geochemistry of the pyrite ores with the mineralogy and crystal-chemistry of phases occurring in late-stage Alpine extension veins hosted in these ore deposits. Accordingly, we have modified the text, made explicit this comparison. Indeed, late-stage veins acted as local drainage systems and their mineralogy mirrors the geochemistry of the host rock. One can reply that hydrothermal fluids could have modified the geochemistry of pyrite ores, by adding some elements. It could be true, but the peculiar geochemistry of pyrite is the same in all the ore deposits studied and some of them (e.g., Fornovolasco, Canale della Radice) were not affected by significant veining. Consequently, we suggest that pyrite ore geochemistry controlled the mineralogy of extension veins and not viceversa.
About the element speciation, we are planning future studies (LA-ICP-MS, XAS, TEM) in order to fully characterize the pyrite chemistry (pyrite and not pyrite ore) and the element speciation in this disulfide.

R: Data about Au content of these pyrites were not reported even if in some cases samples are from epithermal mineralization…what is the reason?

The reasons are discussed above and they are mainly related to analytical issues.

R: Were the samples studied by reflected light microscopy prior to analyses? If yes – completing Table 1 with data on the observed solid inclusions in each sample. It could be of help for the interpretation – trace elements due to solid inclusions vs. fixed in the crystal lattice of the pyrite.

Some information has been added to the text.

R: What about correlations between mono-, di- and trivalent cations other than Tl in the studied samples – As-Sb, Zn-Cd, Co-Ni, Tl-Ag, Pb-Zn etc??? Using mole plots could help discrimination between mineral inclusions and real trace elements in pyrite.

It is not the aim of this paper to discriminate the element speciation in pyrite, because we are studying the pyrite ore and the elemental relationships are probably due to the superposition of inclusions as well as substitutions in the pyrite ore matrix. However, we improved the manuscript using mole plots for several metals (Fig. 9) providing a discussion on element speciation in pyrite ores (trace elements in pyrite versus accessory minerals in the ore sample).

R: Is there any correlation between Pb-isotopes and particular trace element or element ratio that could be used to trace fluid source?

Geological evidences, as well as petrographic, geochemical, and isotopic data indicates a local remobilization of Paleozoic ores probably owing to the action of metamorphic fluids. Indeed, massive ore bodies and late-stage minerals (e.g., sulfides and sulfosalts in Alpine extensional veins) show similar lead isotopic composition.

R: Not only!!! Also epithermal, porphyry deposits, skarns... See a just published paper in American Mineralogist plus a number of papers with LA-ICP-MS data on trace elements in pyrite from various environments published in the last five years or so.

We agree with the reviewer that thallium occurs in several kinds of ore deposits. However, the higher Tl contents (Tl > 500 μg/g) are mainly related to Carlin-type and stratiform basin-hosted sulfide deposits, e.g., up to 1712 μg/g in Carlin-type deposit studied by Scott et al. (2009) or 1166 μg/g in pyrite from sedimentary environments reported by Large et al. (2014). Pyrite from other occurrences usually has lower Tl contents (e.g. up to 321 μg/g in high-sulfidation epithermal deposits described by Scher et al., 2013).

R: Was such transition observed at one particular site or these two mineralization styles occur ALWAYS separated?

As reported in the text, there is a continuous transition between these two mineralization styles that can occur together at the some particular sites (e.g., the Pollone or the Argentiera di Sant'Anna mines).

R: Two different subparallel trends exist on (a), (c), and (d), emplying different Sb/Tl, As/Tl, and Mo/Tl ratios in the studied samples – this need discussion.

The occurrence of subparallel trends seems to be evident only in Sb/Tl and As/Tl plots, whereas it is not so clear in Mo/Tl diagram. Pyrite ores from Apuan Alps share several geochemical and textural features, but probably they are not homogenous as concern the degree of metamorphic recrystallization, in some cases likely triggered by hydrothermal fluid circulation. In addition, these different trends occur not only between different orebodies, but also within a single ore deposit (see for example data points representing pyrite ores from the Pollone mine). Consequently, we do not know if these differences are related to primary features of the orebodies or if these inhomogeneities are related to the Appenine tectono-metamorphic events. Further studies are mandatory to fully address this issue.

Reviewer #2 (Artur Deditius)

R: The reader is briefed about the shortage of the mineralogical data on Tl-minerals in the investigated region/s. In my opinion this crucial information is also not provided in the manuscript.

The aim of the manuscript is the description and discussion of geochemical data related to the pyrite ores. The most interesting feature is probably represented by the high thallium content shown by pyrite ores from southern Apuan Alps; this high content is also reflected in the local presence, in late-stage veins, of thallium minerals. In our opinion, the references given in the text and Figure 4 represent an useful background for the knowledge of Tl-mineralogy in the studied area.

R: There is a report about the complex textures of pyrite in the results section, but no figures showing the actual pyrite/marcasite/sulphides mineralization are provided.

We agree with the reviewer and we added BSE images showing textural features of the investigated samples.

R: I believe that the key question about the mineralogical form of Tl in the investigated samples remains unanswered.

A discussion about the mineralogical form of Tl in the pyrite ore has been added in the text. Thallium speciation in the sample studied is currently under investigation through a multi-technique approach (XAS, TEM, LA-ICP-MS) and it has been only preliminary discussed in the present contribution.

Table 1

Table 1 Details of the Pyrite/marcasite ores from Tuscany analyzed in this study

Sample	*Locality*	*Description*	*Wt% Pyrite /marcasite*
Southern Apuan Alps mining district			
ARS-3	S. Olga level, M. Arsiccio mine	mg Py in dolostone	~75
ARS-4a	S. Olga level, M. Arsiccio mine	mg Py in dolostone	~85
ARS-4b	S. Olga level, M. Arsiccio mine	mg Py in dolostone	~75
ARS-5	S. Olga level, M. Arsiccio mine	mg Py in dolostone	~40
ARS-10	S. Olga level, M. Arsiccio mine	mg Py + Brt	~75
ARS-13	S. Olga level, M. Arsiccio mine	mg Py	~95
ARS-11	Zabelli level, M. Arsiccio mine	mg Py + Brt	~75
ARS-12	Zabelli level, M. Arsiccio mine	mg Py + Brt	~70
ARS-9	S. Anna level, M. Arsiccio mine	mg Py + Brt	~90
ARS-14	Ribasso Pianello II, M. Arsiccio mine	mg Py + Brt + Qtz	~80
BDV-1	Buca della Vena mine	mg Py + Brt	~50
BDV-4	Buca della Vena mine	mg Py + Brt	~50
CDR-1	Canale della Radice mine	mg Py + Po/Mck	> 99
CDR-2	Canale della Radice mine	mg Py + Po/Mck	> 99
CDR-4	Canale della Radice mine	mg Py	> 99
CDR-6	Canale della Radice mine	mg Py	> 99
CDR-7	Canale della Radice mine	mg Py	> 99
POL-1	Pizzone level, Pollone mine	mg Py + Brt	~80
POL-2	Pizzone level, Pollone mine	mg Py + Brt	~70
POL-3	Pizzone level, Pollone mine	mg Py + Brt	~50
POL-8	Preziosa level, Pollone mine	mg Py + Brt	~80
POL-9	Pozzo Francese level, Pollone mine	mg Py + Brt	~85
FOR-1	Cava del Ferro, Fornovolasco mine	mg Py + Mck	> 99
FOR-2	Cava del Ferro, Fornovolasco mine	mg Py	> 99
FOR-3	Cava del Ferro, Fornovolasco mine	mg Py + Mck	> 99
FOR-5	Cava del Ferro, Fornovolasco mine	mg Py	> 99
FOR-7	Fornaccia, Fornovolasco mine	mg Py	> 99
RSB-1	Ribasso S. Barbara, Argentiera mine	mg Py	> 99
RSB-2	Ribasso S. Barbara, Argentiera mine	mg Py + Brt + Po/Mck	~95
FON	Fontana level, Argentiera mine	mg Py + Qtz + “mica”	~70
SEN	Case Sennari Pyrite outcrop	mg Py + Brt	~80
TAN	La Tana mine	mg Py + Qtz + “mica”	~75
Southern Tuscany mining district			
E-CAL	Vallone Basso stope, M. Calamita mine	idiomorphic Py crystals in “chlorite”	> 99
E-BAC	Bacino stope, Rio Marina mine	blocky Py	> 99
E-GIO	Valle Giove stope, Rio Marina mine	blocky Py	> 99
E-FB	Filone Basso stope, Rio Marina mine	mg Py with adularia	~80
E-TN	Terra Nera mine	blocky Py	> 99
E-GV	Ginevro mine	blocky Py in skarn	> 99
BM-1	Botro ai Marmi mine, Campiglia M.ma	blocky Py	> 99
BM-2	Botro ai Marmi mine, Campiglia M.ma	idiomorphic Py crystals in “chlorite”	> 99
TEMP	Level 4, Earle shaft, Temperino mine, Campiglia M.ma	massive Py	> 99
PV105	Level 6, Earle shaft, Temperino mine, Campiglia M.ma	idiomorphic Py crystals in Hd	> 99
MV	Monte Valerio Mine, Campiglia M.ma	blocky Py	> 99
GAV-1	Gavorrano mine	blocky Py with Cal	> 99
GAV-2	Gavorrano mine	blocky Py	> 99
GAV-3	Gavorrano mine	large (3.5 cm) idiomorphic cubic crystal of Py	> 99
NIC-1	Niccioleta mine	idiomorphic cubic crystal of Py	> 99
NIC-2	Niccioleta mine	mg Py	> 99
NIC-3	Niccioleta mine	blocky Py	> 99
CAM-1	Campiano mine	blocky Py	> 99
CAM-2	Campiano mine	blocky Py	> 99
FBOC	Filone Boccheggiano	mg Py	> 99
BOC	Baciolo stope, Boccheggiano mine	mg Py	> 99
FC A2	Fenice Capanne mine	idiomorphic cubic crystal of Py	> 99
FC B	Fenice Capanne mine	mg Py	> 99
GCAMP	Campese mine, Giglio Island	mg Py	> 99
ABB	Abbadia San Salvatore mine	idiomorphic Mrc crystals with Cn	> 99
BAG	Bagnore mine	idiomorphic Mrc crystals	> 99
PIE	Pietrineri mine	mg Mrc	> 99
LAB	Monte Labro mine	idiomorphic Mrc crystals	> 99
SIE-1	Siele mine	idiomorphic Mrc crystals	> 99
SIE-2	Siele mine	idiomorphic Py crystals	> 99
TAF	Tafone mine	nodule of fibrous-radiate Py in carbonate breccia	> 99

Abbreviations: Brt, baryte; Cal, calcite; Cn, cinnabar; Hd, hedenbergite; Mck, mackinawite; mrc, marcasite, Py, pyrite; Po, pyrrhotite; Qtz, quartz; mg, microgranular.

Table 2

Table 2 Analytical isotopes, operation mode, and detection limits (µg/g in the solid sample) for ICP-MS analyses

Element	*Analyte isotope (mass number)*	*Operation mode*	*Detection Limit (µg/g)*
V	51	KED	0.02
Mn	55	STD	0.08
Co	59	STD	0.01
Ni	60	STD	0.1
Cu	63	STD	0.9
Zn	66	STD	1
As	75	KED	1
Mo	98	STD	0.7
Ag	107	STD	0.01
Cd	111	STD	0.01
Sb	121	STD	0.01
Tl	205	STD	0.01
Pb	206, 207, 208	STD	0.06
Internal Standards			
Rh	103	KED/STD	
Re	187	STD	

Abbreviations: KED, kinetic energy discrimination mode; STD, standard mode.

Table 3

Table 3 Trace-element analyses of pyrite ores from the southern Apuan Alps. Concentrations in µg/g

Sample	*Locality*	***Tl***	*V*	*Mn*	*Co*	*Ni*	*Cu*	*Zn*	*As*	*Mo*	*Ag*	*Cd*	*Sb*	*Pb*
ARS-3	Monte Arsiccio mine	**206**	8.1	< d.l.	1.69	43	11.2	40	238	16.6	6.4	0.44	2430	90
ARS-4a	Monte Arsiccio mine	**159**	2.37	< d.l.	1.45	28.1	14.1	30.0	282	17.9	5.9	0.85	626	279
ARS-4b	Monte Arsiccio mine	**162**	11.8	< d.l.	3.6	40	10.2	48	268	14.5	5.6	0.54	1060	218
ARS-5	Monte Arsiccio mine	**97**	134	< d.l.	1.73	24.1	12.8	248	105	1.34	5.6	0.81	631	25.6
ARS-10	Monte Arsiccio mine	**258**	16.6	23.4	0.99	56	2.95	13.0	180	16.6	44	0.67	534	39
ARS-13	Monte Arsiccio mine	**393**	8.5	25.0	21.0	35	13.2	63	451	23.1	29.8	0.59	802	198
ARS-11	Monte Arsiccio mine	**192**	20.1	23.8	5.9	27.3	99	34	232	6.0	3.26	0.25	442	72
ARS-12	Monte Arsiccio mine	**194**	64	18.2	3.17	37	7.3	121	172	23.0	14.4	1.23	314	69
ARS-9	Monte Arsiccio mine	**110**	1.04	103	0.62	9.4	16.2	206	148	14.2	34	1.33	1090	182
ARS-14	Monte Arsiccio mine	**77**	2.82	27.6	1.81	72	10.7	28.0	640	8.2	0.68	0.09	88	171
BDV-1	Buca della Vena mine	**82**	24.6	< d.l.	9.5	148	47	4.8	225	15.1	48	0.90	224	24.1
BDV-4	Buca della Vena mine	**124**	252	12.6	25.2	97	9.1	12.2	127	14.5	0.16	0.07	278	11.1
CDR-1	Canale della Radice mine	**460**	248	< d.l.	36	400	105	20.5	416	45	1.77	0.73	335	47
CDR-2	Canale della Radice mine	**576**	779	< d.l.	15.9	251	79	176	1420	21.0	0.27	1.13	419	26.9
CDR-4	Canale della Radice mine	**437**	288	78	13.9	194	16.7	< d.l.	1450	42	1.71	0.14	828	108
CDR-6	Canale della Radice mine	**1030**	147	73	9.5	458	104	37	808	29.9	4.2	0.40	1400	69
CDR-7	Canale della Radice mine	**871**	165	68	3.6	216	34	48	1170	42	1.72	0.47	1120	90
POL-1	Pollone mine	**10.5**	0.96	6.8	10.7	61	53	610	151	13.7	57	2.57	91	405
POL-2	Pollone mine	**156**	12.1	18.6	2.84	17.6	47	99	198	1.80	31.2	0.92	168	381
POL-3	Pollone mine	**15.5**	4.0	366	0.71	24.4	24.1	129	202	9.0	18.0	0.27	135	438
POL-8	Pollone mine	**76**	17.5	2.08	3.26	29.6	7.6	711	127	1.33	30.8	0.14	107	18.8
POL-9	Pollone mine	**640**	3.8	71	4.6	25.2	101	744	1980	4.8	18.4	3.7	1140	1810
FOR-1	Fornovolasco mine	**888**	52	29.6	25.6	166	4.2	57	1240	21.3	0.43	0.57	1950	155
FOR-2	Fornovolasco mine	**758**	8.3	19.6	45	190	16.4	450	1620	59	1.16	1.86	1750	200
FOR-3	Fornovolasco mine	**923**	84	38	34	242	13.9	103	1250	21.9	0.87	0.83	1890	110
FOR-5	Fornovolasco mine	**1110**	3.00	21.2	62	175	3.7	3.5	1470	56	0.69	0.97	1970	158
FOR-7	Fornovolasco mine	**677**	109	127	17.6	90	28.6	5.0	2120	28.3	5.0	0.61	1260	303
RSB-1	Argentiera di Sant'Anna mine	**31.2**	97	2270	0.41	89	75	95	228	72	0.81	0.13	67	12.0
RSB-2	Argentiera di Sant'Anna mine	**91**	3.3	7.9	0.41	189	9.7	19.7	988	25.1	5.7	0.11	178	13.0
FON	Argentiera di Sant'Anna mine	**17.6**	36	12.1	21.2	213	150	185	972	2.25	25.2	1.67	354	10320
SEN	Sant'Anna di Stazzema	**624**	11.2	32.1	22.1	134	12.5	91	317	26.9	0.81	0.36	722	44
TAN	La Tana mine	**115**	12.7	2.35	7.5	50	10.8	204	1010	2.23	38	3.8	775	541

Abbreviations: < d.l., below detection limit.

Table 4

Table 4 Lead isotope compositions for pyrite ores and lead sulfides and sulfosalts from the southern Apuan Alps

Sample	*Locality*	*Material*	$^{208}Pb/^{204}Pb$	*2s*	$^{207}Pb/^{204}Pb$	*2s*	$^{206}Pb/^{204}Pb$	*2s*
BDV-1	Buca della Vena mine	bulk mc pyrite-baryte ore	38.5398	0.0052	15.6725	0.0031	18.4033	0.0015
BV-Gn1	Buca della Vena mine	fg galena	38.5267	0.0060	15.6702	0.0028	18.3897	0.0013
CDR-7	Canale della Radice mine	bulk mc pyrite ore	38.5427	0.0043	15.6717	0.0025	18.3321	0.0011
FOR-5	Cava del Ferro mine	bulk mc pyrite ore	38.5671	0.0050	15.6778	0.0027	18.4223	0.0014
F-J-4141	Cava del Ferro mine	idiomorphic jamesonite	38.5450	0.0039	15.6735	0.0034	18.4303	0.0015
P-Py1	Pozzo Francese level, Pollone mine	bulk mc pyrite-baryte ore	38.5363	0.0043	15.6742	0.0033	18.3589	0.0017
P-Gn1	Pozzo Francese level, Pollone mine	fg galena	38.5154	0.0043	15.6690	0.0030	18.3132	0.0016
P-Gn2	Preziosa level, Pollone mine	cg galena	38.5496	0.0061	15.6639	0.0029	18.3444	0.0019
A-Py1	Fontana level, Argentiera mine	bulk mc pyrite ore	38.5211	0.0054	15.6672	0.0027	18.3523	0.0016
A-Gn1	Fontana level, Argentiera mine	fg galena	38.5517	0.0040	15.6713	0.0025	18.3391	0.0014
MA-Z	S. Olga level, Monte Arsiccio mine	idiomorphic zinkenite	38.5862	0.0048	15.6730	0.0026	18.3676	0.0016
MA-R-19443	S. Olga level, Monte Arsiccio mine	idiomorphic rouxelite	38.5850	0.0045	15.6735	0.0028	18.4092	0.0017
Pchab-B	S. Olga level, Monte Arsiccio mine	protochabournéite in baryte	38.6103	0.0055	15.6754	0.0032	18.4157	0.0012
Pchab-D	S. Olga level, Monte Arsiccio mine	protochabournéite in dolostone	38.5924	0.0043	15.6746	0.0026	18.4006	0.0011
MA-Gn1	Cascatoia, Monte Arsiccio area	fg galena	38.5723	0.0057	15.6756	0.0031	18.3867	0.0015
MA-Gn2	Monte Arsiccio area	fg galena	38.5487	0.0052	15.6732	0.0023	18.3798	0.0018
B-Gn1	Bottino mine	cg galena	38.4821	0.0038	15.6622	0.0027	18.3089	0.0012
B-Gn2a	Bottino mine	fg galena	38.5009	0.0048	15.6683	0.0031	18.3378	0.0012
B-Gn2b	Bottino mine	cg galena	38.5120	0.0041	15.6712	0.0022	18.3148	0.0014
B-Gn2c	Bottino mine	idiomorphic galena	38.5181	0.0050	15.6732	0.0026	18.3320	0.0016

Abbreviations: mc, microcrystalline; fg, fine-grained; cg, coarse-grained

Table 5

Table 5 Trace-element analyses of pyrite/marcasite ores from southern Tuscany. Concentrations in µg/g

Sample	*Locality*	***Tl***	*V*	*Mn*	*Co*	*Ni*	*Cu*	*Zn*	*As*	*Mo*	*Ag*	*Cd*	*Sb*	*Pb*
E-CAL	Monte Calamita mine	**0.04**	0.47	40	1130	13.0	3010	114	389	< d.l.	1.23	0.23	0.39	5.0
E-BAC	Rio Marina mine	**0.01**	3.5	4.8	6020	174	2.56	30.7	348	3.4	0.09	0.01	0.19	9.9
E-GIO	Rio Marina mine	**0.06**	0.03	6.4	0.63	< d.l.	11.2	1.19	2080	< d.l.	0.06	< d.l.	0.26	1.05
E-FB	Rio Marina mine	**0.10**	0.20	4.4	1770	37	0.96	< d.l.	479	< d.l.	0.16	< d.l.	0.17	0.44
E-TN	Terranera mine	**0.26**	0.03	5.5	616	59	3.7	< d.l.	158	< d.l.	< d.l.	< d.l.	1.35	0.28
E-GV	Ginevro mine	**0.04**	3.7	93	208	1.82	4.5	29.4	64	1.77	0.26	0.03	3.24	9.6
BM-1	Botro ai Marmi	**2.20**	0.70	109	115	15.6	1380	587	752	1.67	5.3	3.5	44	150
BM-2	Botro ai Marmi	**0.04**	< d.l.	7.6	117	46	5.2	4.6	3450	0.80	4.9	0.04	1.69	167
TEMP	Temperino mine	**0.09**	0.63	1120	141	0.88	461	991	319	< d.l.	2.29	2.76	8.0	1120
PV105	Temperino mine	**0.35**	< d.l.	152	19.5	< d.l.	5.8	405	460	< d.l.	3.00	1.06	1.26	127
MV	Monte Valerio mine	**0.12**	1.71	17.1	1.03	5.7	1060	41	2500	< d.l.	1.98	0.23	15.5	88
GAV-1	Gavorrano mine	**0.53**	1.10	629	119	1.38	51	29.4	1950	< d.l.	14.2	0.16	6.9	748
GAV-2	Gavorrano mine	**0.04**	0.35	1.53	197	0.68	22.9	14.3	416	< d.l.	0.74	< d.l.	0.28	20.6
GAV-3	Gavorrano mine	**0.08**	0.34	2.55	42	0.76	< d.l.	21.6	27	< d.l.	1.74	0.04	0.34	2.07
NIC-1	Niccioleta mine	**0.09**	1.12	1.60	166	< d.l.	< d.l.	23.1	23.5	< d.l.	0.08	< d.l.	0.44	5.0
NIC-2	Niccioleta mine	**0.09**	0.72	97	816	8.2	< d.l.	48	59	1.48	0.91	0.05	1.24	23.4
NIC-3	Niccioleta mine	**0.04**	1.35	360	261	3.11	7.5	11.4	102	< d.l.	5.1	0.02	3.4	67
CAM-1	Campiano mine	**0.16**	0.06	82	281	0.16	24.7	2110	207	< d.l.	1.99	7.5	2.15	568
CAM-2	Campiano mine	**0.10**	1.96	469	1418	4.8	12.8	21.0	502	3.11	4.7	0.05	2.50	83
FBOC	Boccheggiano	**0.20**	3.14	5.1	651	1.58	20.4	28.4	2400	< d.l.	5.8	0.02	1.90	27.9
BOC	Boccheggiano	**0.05**	0.12	7.7	38	0.45	45	260	510	< d.l.	1.18	0.56	0.45	40
FC A2	Fenice Capanne mine	**0.27**	11.7	176	40	79	731	60	206	0.95	3.23	0.10	4.3	86
FC B	Fenice Capanne mine	**0.11**	0.68	20.5	23.7	17.4	390	4045	550	< d.l.	25.4	11.0	1.61	1280
GCAMP	Campese mine	**0.12**	4.7	65	80	3.03	16.2	20.2	164	2.12	0.47	< d.l.	0.72	15.3
ABB	Abbadia S. Salvatore mine	**80**	< d.l.	41	0.33	49	< d.l.	134	197	2.00	< d.l.	1.20	< d.l.	27.7
BAG	Bagnore mine	**0.11**	2.87	16.5	1.33	0.31	5.4	137	238	1.10	0.64	0.16	75	5.6
PIE	Pietrineri mine	**201**	0.16	10.7	0.16	6.8	< d.l.	113	570	0.96	1.11	0.43	0.43	8.0
LAB	Monte Labro mine	**24.4**	< d.l.	5.4	2.18	133	< d.l.	9.2	303	33	0.14	0.35	0.33	18.6
SIE-1	Siele mine	**252**	0.57	14.3	0.22	11.8	3.9	156	559	< d.l.	1.17	0.45	0.90	12.9
SIE-2	Siele mine	**0.70**	4.7	75	0.21	< d.l.	2.28	90	15.4	< d.l.	1.45	< d.l.	0.49	5.1
TAF	Tafone mine	**3880**	0.23	38	< d.l.	< d.l.	< d.l.	77	68000	1.12	0.78	< d.l.	4540	< d.l.

Abbreviations: < d.l., below detection limit.

Figure 1

Click here to download Figure Fig.1.tif

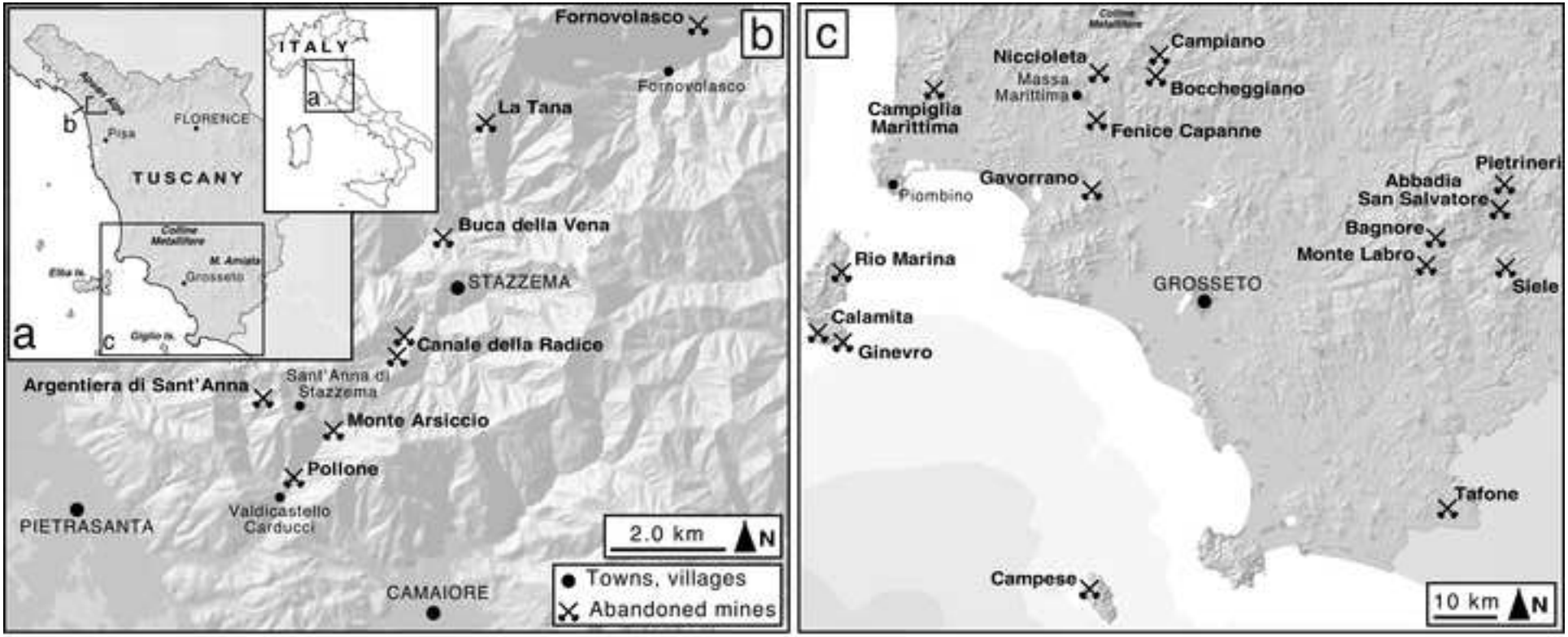

Fig. 1

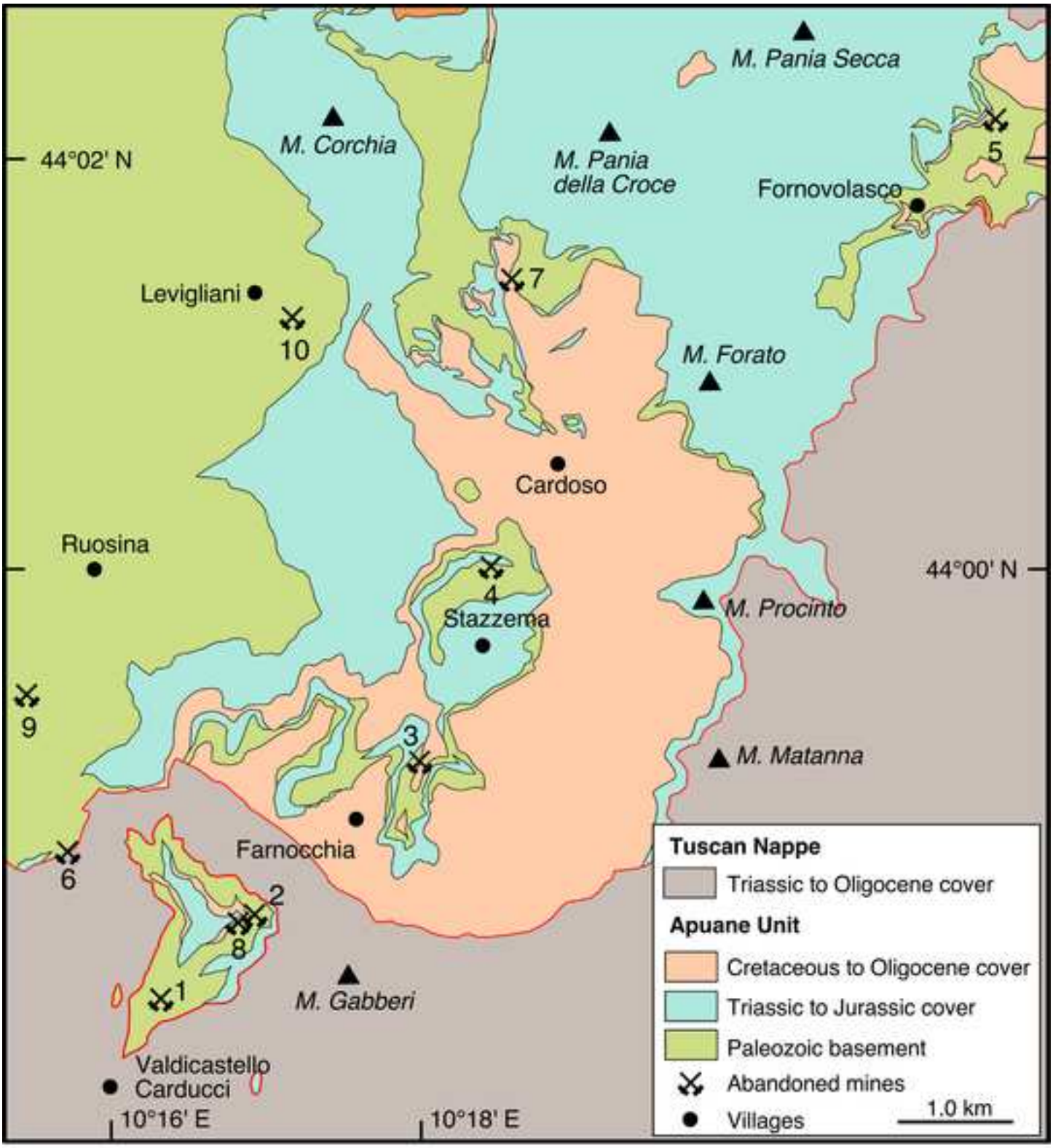

Fig. 2

Figure 3

Click here to download Figure Fig.3.tif

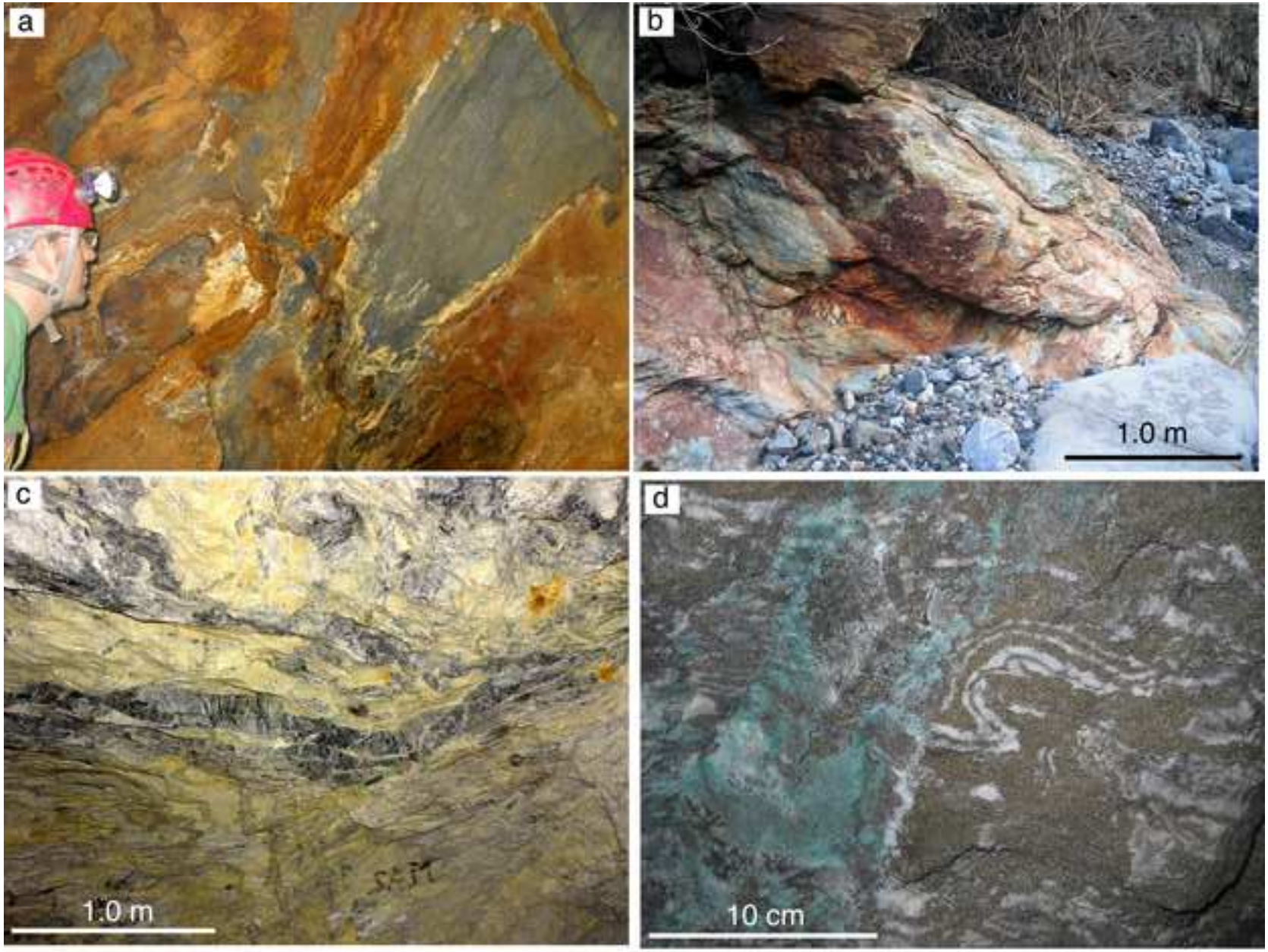

Fig. 3

Figure 4

Click here to download Figure Fig.4.tif

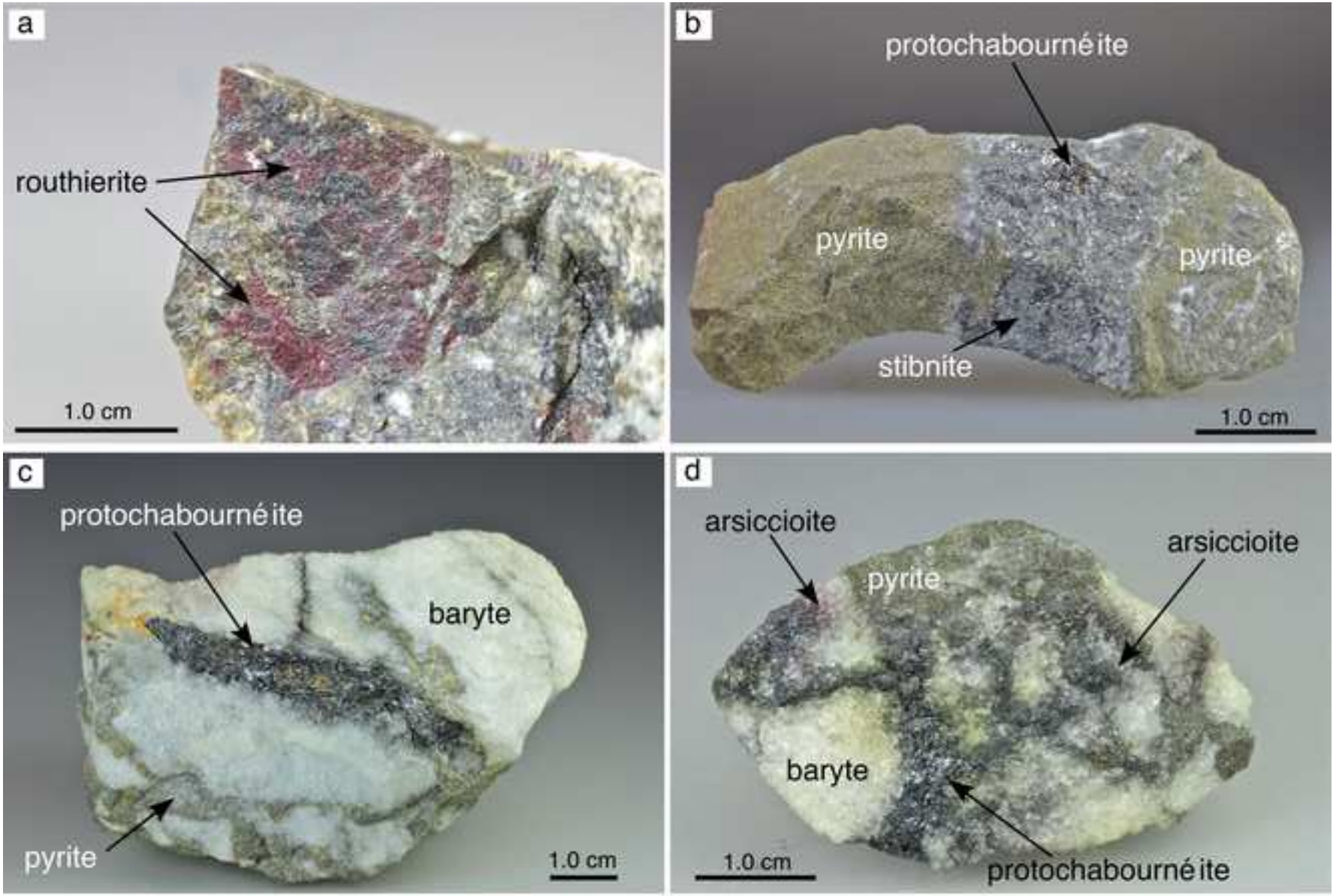

Fig. 4

Figure 5

Click here to download Figure Fig.5.tif

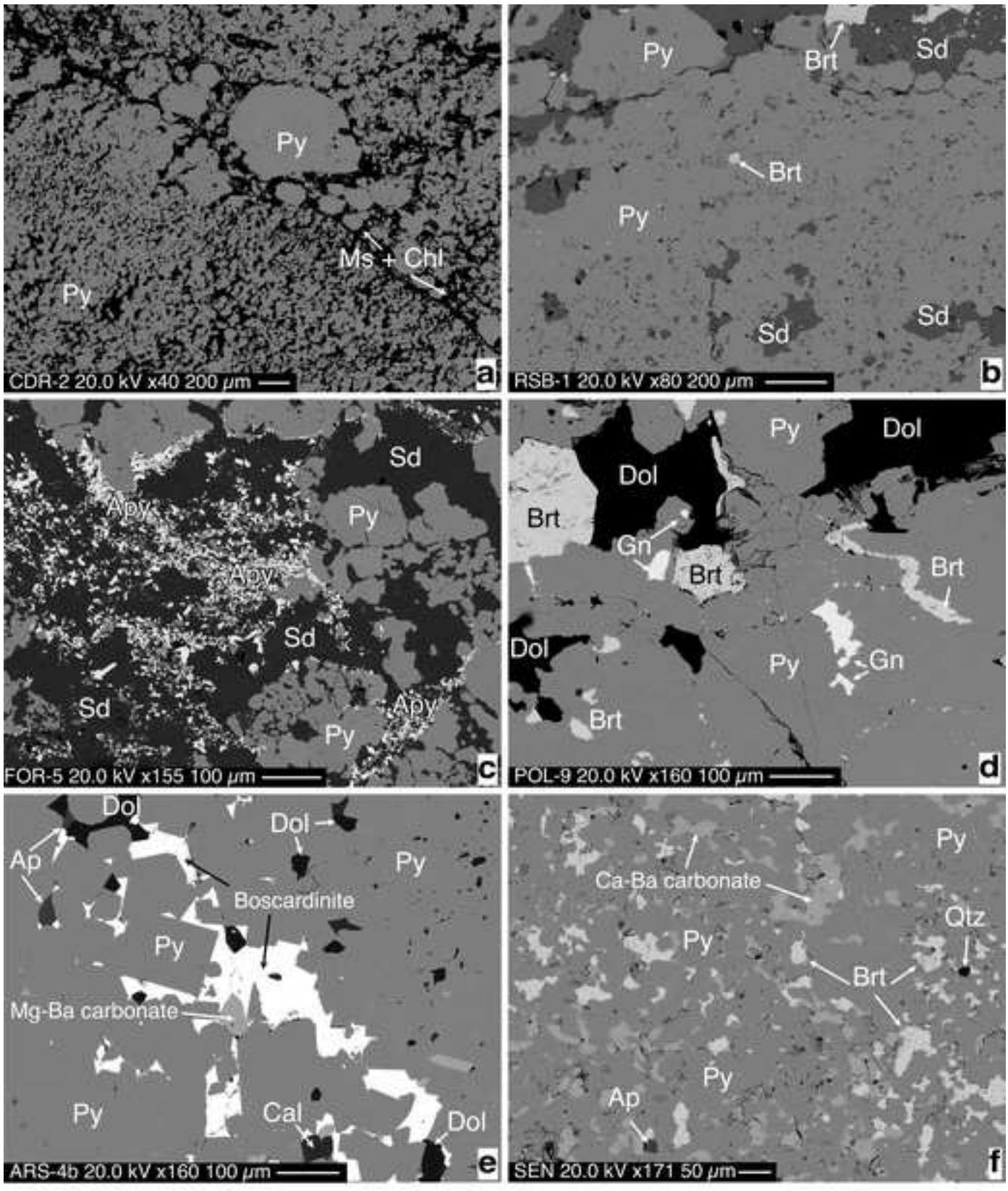

Fig. 5

Figure 6

Click here to download Figure Fig.6.tif

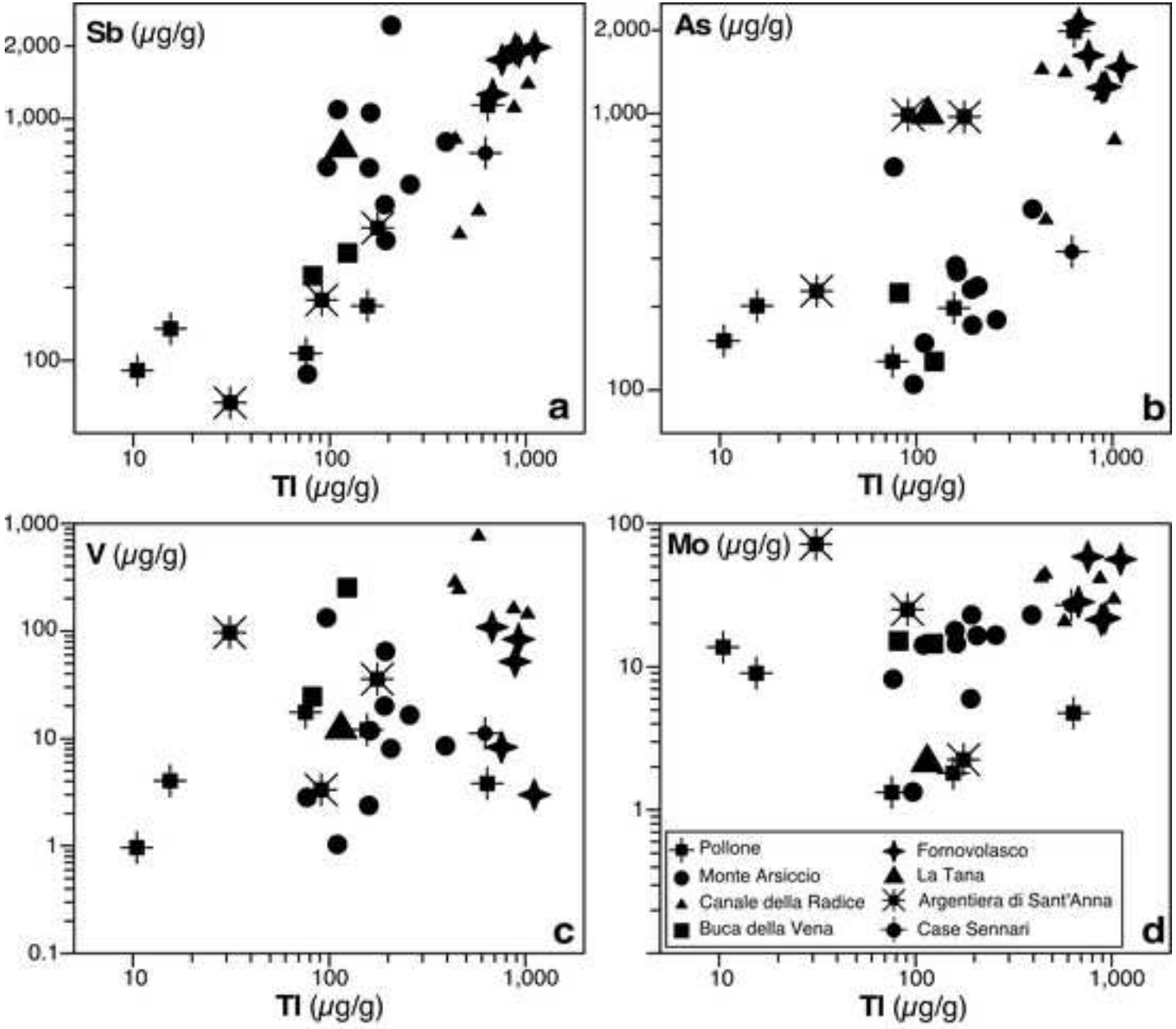

Fig. 6

Figure 7

Click here to download Figure Fig.7.tif

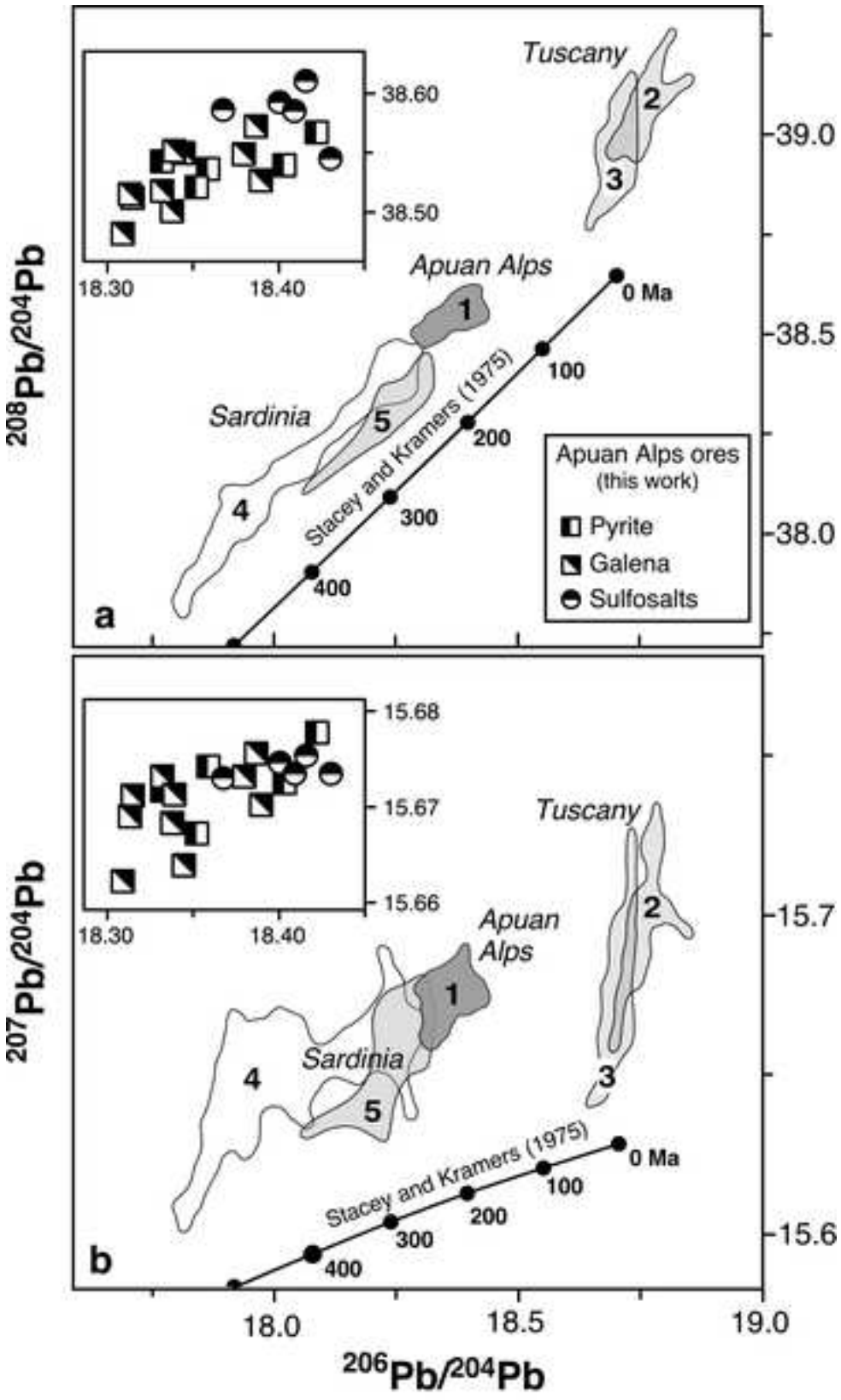

Fig. 7

Figure 8

Click here to download Figure Fig.8.tif

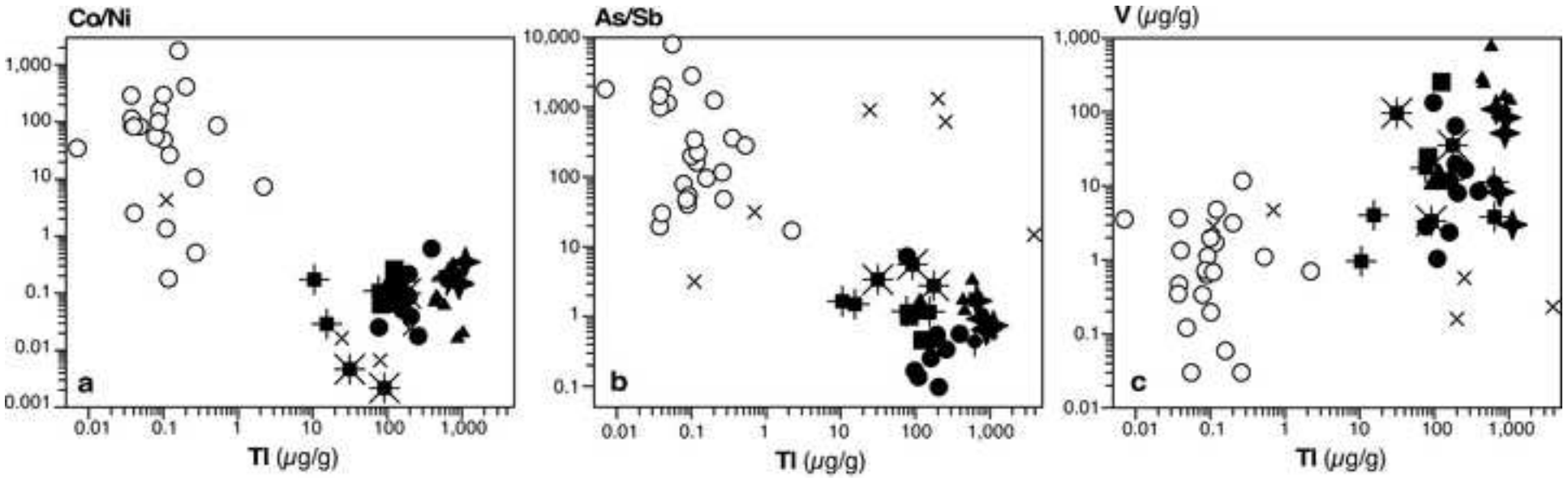

Fig. 8

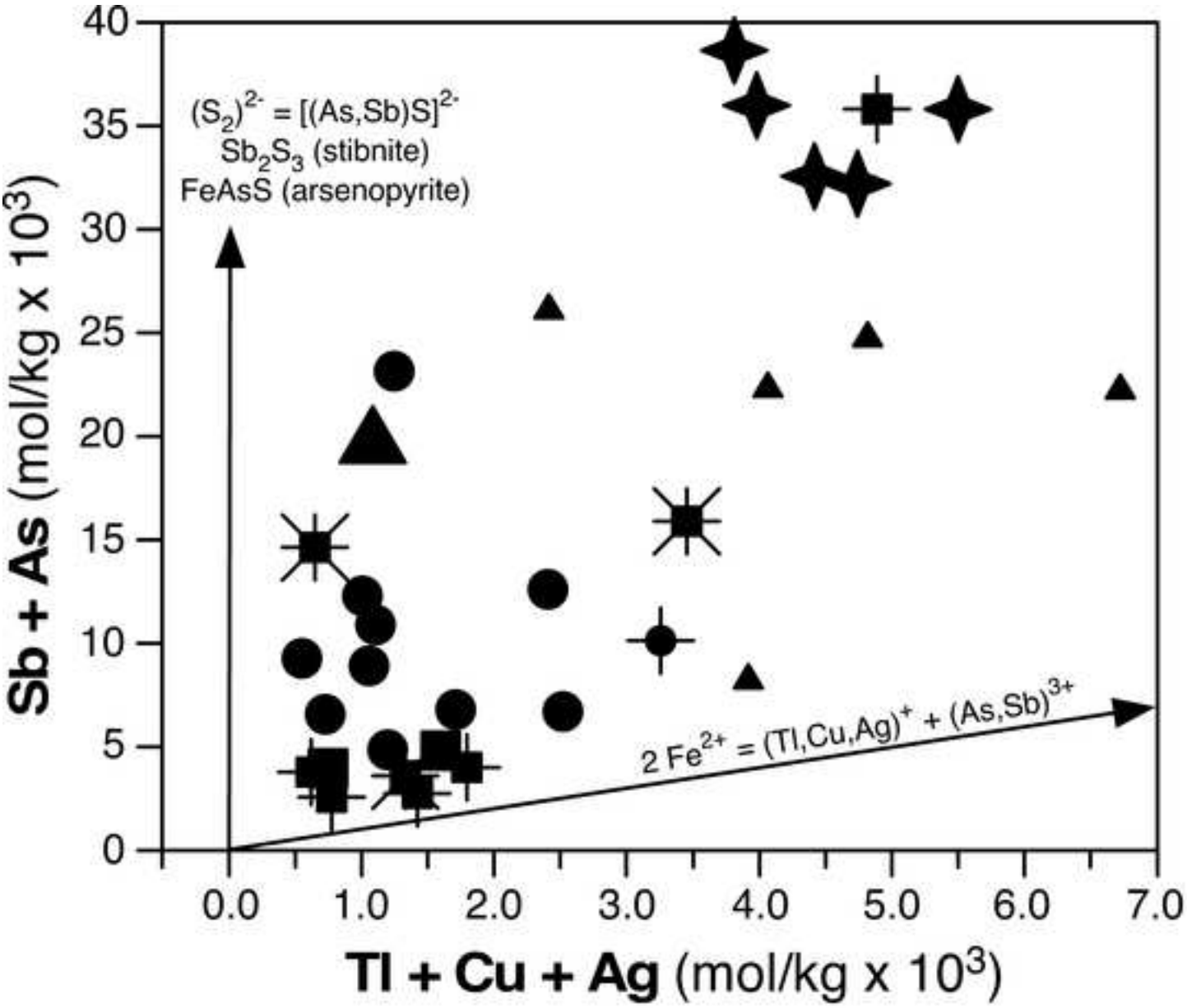

Fig. 9

Figure 10

Click here to download Figure Fig.10.tif

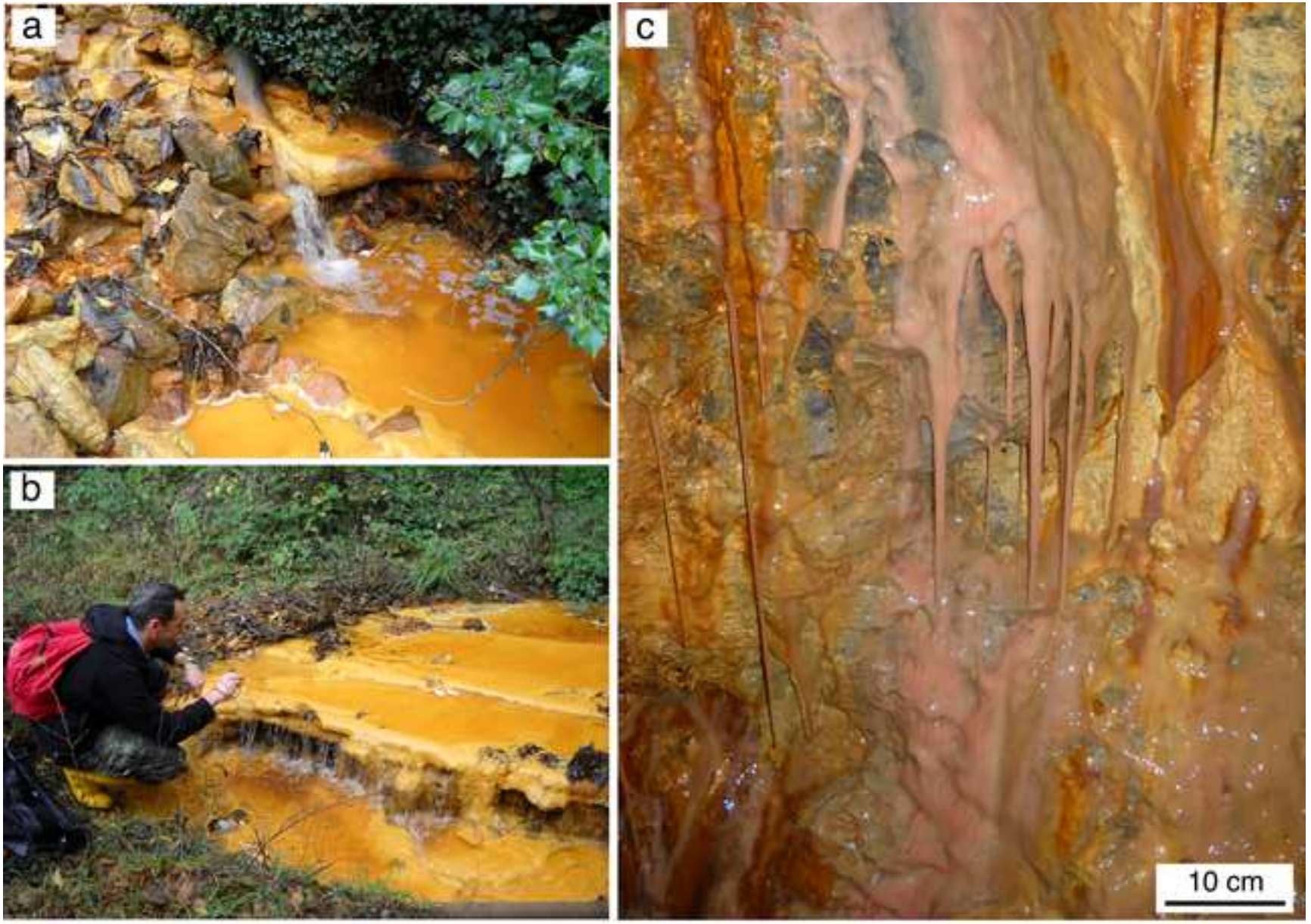

Fig. 10